Removal of Methylene Blue Dye from Aqueous Solution using Magnetite Impregnated Khat Stem Nanocellulose Composites

Hana Melese Berta

A Thesis Submitted to Department of Applied Chemistry,

School of Applied Natural Science

In partial fulfillment of the Requirements for the Degree of Master of Science in Applied Chemistry (Analytical Chemistry)

Office of Graduate Studies

Adama Science and Technology University

June, 2024

Adama, Ethiopia

Removal of Methylene Blue Dye from Aqueous Solution using Magnetite Impregnated Khat Stem Nanocellulose Composites

Hana Melese Berta

Advisor: Aschalew Tadesse (PhD)

Co-Advisor: Hizkeal Tsade (PhD)

A Thesis Submitted to Department of Applied Chemistry, School of Applied Natural Science

In partial fulfillment of the Requirements for the Degree of Master of Science in Applied Chemistry (Analytical Chemistry)

Adama Science and Technology University

Office of Graduate Studies

June, 2024

Adama, Ethiopia

DECLARATION

I hereby declare this MSc thesis entitled "**Removal of Methylene Blue Dye from Aqueous Solution using Magnetite Impregnated Khat Stem Nanocellulose Composites**" is my original research work. That is, it has not been submitted to the Department of Applied Chemistry or any other institute for graduation or any research case. All the materials and methods used in this thesis have been duly acknowledged through appropriate citations**.**

Hana Melese Berta	___________________	____________________
Name of Student	Signature	Date

RECOMMENDATION

We, the advisor(s) of this thesis, hereby certify that we have read the revised version of the thesis entitled "**Removal of Methylene Blue Dye from Aqueous Solution using Magnetite Impregnated Khat Stem Nanocellulose Composites**" prepared under our guidance by Hana Melese submitted in partial fulfillment of the requirements for the degree of Master of Science in Chemistry (Analytical Chemistry). Therefore, we recommend the submission of a revised version of this thesis to the department following the applicable procedures.

Aschalew Tadesse (PhD) ____________________ ____________________

Major-Advisor Signature Date

Hizkeal Tsade (PhD) ____________________ ____________________

Co-advisor Signature Date

LETTER OF APPROVAL

we, the advisors of the thesis entitled "**Removal of Methylene Blue Dye from Aqueous Solution using Magnetite Impregnated Khat Stem Nanocellulose Composites**" and developed by Hana Melese hereby certifies that the recommendation and suggestions made by the board of examiners are appropriately incorporated into the last version of the thesis.

Aschalew Tadesse (PhD)	______________________	________________________
Major Advisor	Signature	Date
Hizkeal Tsade (PhD)	______________________	________________________
Co-advisor	Signature	Date

APPROVAL OF BOARD OF REVIEWERS

We, the undersigned, members of the Board of Reviewers of the thesis open defense by Hana Melese have read and evaluated the thesis entitled "**Removal of Methylene Blue Dye from Aqueous Solution using Magnetite Impregnated Khat Stem Nanocellulose Composites**" and assessed the understanding of the candidate about the thesis. This is, therefore, to certify that the thesis is accepted and we recommend the implementation of the thesis.

___________________________	_________________	__________________
Chairperson	Signature	Date
___________________________	_________________	__________________
Reviewer 1	Signature	Date
___________________________	_________________	__________________
Reviewer 2	Signature	Date

Final approval and acceptance of the thesis is contingent upon submission of its final copy to the Office of Postgraduate Studies (OPGS) through the Department Graduate Council (DGC) and School Graduate Committee (SGC).

_______________________	_____________________	________________
Department Head	Signature	Date
_______________________	_____________________	________________
School Dean	Signature	Date
_______________________	_________________	_____________
Office of Postgraduate Studies, Dean	Signature	Date

ACKNOWLEDGMENT

Above all, I am profoundly thankful to the Almighty God for granting me the good health, fortitude, and patience required to carry out my thesis work. Secondly, I would like to extend my heartfelt gratitude to my advisor, Dr. Aschalew Tadesse, and co-advisor, Dr. Hizkeal Tsade, for their unwavering support and invaluable direction throughout the course of my thesis research. Thirdly, my thanks go to Adama Science and Technology University Department of Applied Chemistry, all academic, technical (Mr. Guta Amanu, and Mr. Girma Hailu), and supporting staff (Mr. Enyew Tilahun) for their support in my thesis work. Fourthly, Also I would like to thank material science laboratory technical Mr. Demeke Tessfaye and all the M.Sc. students. Lastly, I would like to express my heartfelt gratitude to all of my family members and close friends for their unwavering encouragement and support throughout the course of this research endeavor.

TABLE OF CONTENTS

LIST OF FIGURES

LIST OF TABLES

LIST OF ABBREVIATIONS AND ACRONYMS

AA	Acetic Acid
BET	Brunauer, Emmett and Teller
CNC	Cellulose Nanocrystals
Cs	Cellulose
DSC	Differential Scanning Calorimetry
FA	Formic Acid
FTIR	Fourier Transforms Infrared
KW	Khat Waste
MB	Methylene Blue Dye
MNC	Magnetite Impregnated Nanocellulose Composites
NC	Nanocellulose
RNA	Ribonucleic Acid
SEM	Scanning Electron Microscopy
UV-Vis	UV-Visible Spectroscopy
XRD	X-ray Diffraction

ABSTRACT

The increased development of industrial, urban, and agricultural activities around the world is primarily responsible for the remove of different contaminants, including hazardous heavy metals, nutrients, dyes, etc., into aquatic environments. This study focused on the synthesis and characterization of nanocellulose derived from Khat stems, which was then impregnated with magnetite to form composite materials. The aim was to investigate the removal of methylene blue (MB) dye from aqueous solutions using these composite adsorbents. Magnetite impregnated nanocellulose composite (MNC) was synthesized by the coprecipitation method of nanocellulose with two iron oxides ($FeCl_2$ and $FeCl_3$) and characterized using phase transitions by Differential Scanning Calorimetry (DSC), crystallography by X-ray Diffraction (XRD), Functional groups by Fourier Transforms Infrared (FTIR), morphology by Scanning Electron Microscopy (SEM), and Surface area by Brunauer, Emmett and Teller (BET). The MNC was more thermally stable than nanocellulose. The XRD spectra of MNC exhibited peaks at 2θ 16.6° and 22.6° which are supposed to represent the typical cellulose I structure and at 2θ of 18.4°, 30.4°, 35.5°, 43.2°, 53.9°, 57.2°, 62.8°, and 74.2° indicating the structure of magnetite iron oxide nanoparticles. The BET multi point surface area, average pore size, and total pore volume of MNC were 511.74 m^2/g, 0.619 nm, and 1.335 cc/g, respectively. Batch adsorption experiments were conducted to examine the influence of various parameters, including pH, contact time, adsorbent dose and initial dye concentration, on the sorption of MB dye. The maximum MB dye removal efficiency was 97%, which was achieved at a pH of 8, an initial MB dye concentration of 10 mg/L, an adsorbent dosage of 0.07 g/100mg/L, and a contact time of 80 minutes. The adsorption mechanisms were more closely aligned with Langmuir isotherm model than Freundlich model, demonstrating a maximum adsorption capacity of 102.35 mg/g and a R^2 of 0.996. The kinetics of the adsorption process was well described by the pseudo second order kinetic model, which achieved a high R^2 of 0.996. The reusability test was investigated using a single sample weighing 0.07 g/100mL for five cycles, and up to 88.97% of methylene blue was eliminated. It has been observed that magnetite impregnated khat stem based nanocellulose composites has great adsorption capabilities for removing MB dye from an aqueous solution.

Keywords: Adsorption, Aqueous Solution, Composite, MB Dye, Magnetite, Nanocellulose, Magnetite Impregnated Nanocellulose

CHAPTER ONE

1. INTRODUCTION

1.1. Background

Globally, one of significant environmental problems is water pollution (Tsade et al., 2021). Numerous companies release wastewater that contains colors and heavy metals, which severely harms the aquatic ecosystem (Kamaraj et al., 2020). Because of their toxicity, trophic chain movement, chemical stability, and challenges to purification, the heavy metals and organic dyes found in wastewater have been identified as hazardous to the ecological system (Jaishankar et al., 2014). Many synthetic organic dyes are derived from petrochemical sources and can have significant negative environmental and health impacts. Some organic dyes are persistent, bioaccumulative, and toxic, posing risks to aquatic ecosystems and human health if improperly managed or disposed of (Ismail et al., 2019).

In particular, it is well established that methylene blue (MB) dye, which is found in polluted water from numerous industries such as textile, dyeing, printing, cosmetics, paper making, and food coloring, is carcinogenic and detrimental to living organisms. Despite the significance of this dye in science, it can cause dangerous effects on living things and the environment because of water solubility nature of MB dye. These causes include mutations, allergic dermatitis, cancer, and irritation of the skin (Tsade et al., 2021; Senthil Kumar et al., 2014). Therefore, it is crucial to remove these types of dyes that produce toxins from the aqueous system before the wastewater is discharged into the environment.

Conventional methods for dye removal, such as chemical precipitation, membrane filtration, and biological treatment, have had limited success, particularly when dealing with recalcitrant dyes like methylene blue (Zhou et al., 2019). Adsorption is the most powerful methods for removing dyes. The main downside of this approach was the high cost of the adsorbents used. However, with the development of low cost adsorbents that are equally effective, adsorption now becomes a cost effective way to remove dyes across the globe (Katheresan et al., 2018). Among various processing technologies, adsorption is widely regarded as the superior choice due to its cost-effectiveness, flexibility, simple design, ease of operation, and ability to handle hazardous pollutants (Sardar et al., 2021). This process is highly efficient, cost-effective, and can achieve high removal rates compared to traditional techniques. Ongoing research is focused on developing advanced adsorbent materials and optimizing adsorption conditions to further enhance the remediation of methylene blue dye.

Nanocellulose is a natural polymer material, with at least one of its dimensions falling within nanoscale range. It can be obtained in substantial quantities from the natural environment, as it derived from different cellulosic materials like wood, agricultural waste and certain type of bacteria. It is biodegradable, has low density, low porosity, and a higher surface area. Additionally, it is fairly inexpensive to manufacture, making it a cost efficient option for different applications. Nanocellulose, which is derived from cellulose fibers, lacks inherent magnetic properties, due to this properties it need modification. when NC is combined with magnetite, it possess unique magnetic properties (Nypelö, 2022). Magnetite impregnated with nanocellulose composites has unusual magnetic characteristics, making it a versatile and promising material for a wide range of applications. These include environmental cleanup, such as the removal of heavy metals and dyes from water; biomedical engineering, such as medication delivery and tissue engineering; and electronics, where it is employed in magnetic sensors and data storage devices (Kumar et al., 2021).

The magnetite on the nanocellulose increases the magnetic properties, strength, reusability, and surface area of the nanocellulose materials (Zhao et al., 2020). To prevent pollution of the environment, renewable natural resources are attracting a lot of attention nowadays for the production of recyclable and/or biodegradable items. One of the most significant natural resources for the synthesis of biopolymers or value added materials is lignocellulosic material (Arevalo Gallegos et al., 2017). Khat stem is one of the agricultural wastes that can be used for the preparation of nanocellulose (Gabriel et al., 2021). To the knowledge of the author, no research work was reported on the preparation and characterization of a khat stem based nanocellulose magnetite composite used for the removal of methylene blue dye from an aqueous solution. This thesis was focused on the preparation and characterization of a magnetite impregnated nanocellulose composite adsorbent for the removal of cationic MB dye.

1.2. Statement of the Problem

In Ethiopia, from the increasing human population, uncontrolled urbanization and inadequate sanitation infrastructure cause serious quality degradation of surface waters. Although rapid industrial expansion is viewed as an indicator of economic progress, they are greatly associated with environmental degradation, particularly due to the discharge of untreated wastewater into the aquatic environment. There are several industries found in Ethiopia such as, tanneries, textiles, metals, minerals, glass, beverages, etc. Among these, especially, the operation of tanneries and textiles are causing severe environmental pollution due to the disposal of untreated effluent on land and in water bodies in large amount (Yohannes & Elias, 2017).

MB is one of the most thoroughly studied dyes due to its both positive and negative aspects. It has extensive and broad applications as coloring and staining agent in the textile and pharmaceutical sectors, respectively. However, MB has attracted serious attention due to its hostile nature, which poses inharmonious effects on the environment and human health. High blood pressure, irritation of the skin with redness and itching, irritation of throat, mouth, esophagus, and stomach, gastrointestinal pain, nausea, vomiting, diarrhea, dizziness, headache, and fever are some general problems associated with this dye (Mashkoor & Nasar, 2020). The elimination of colors from wastewater effluents can be achieved by various techniques (Yuan et al., 2019). For the removal of methylene blue (MB) dye, the adsorption method is considered the most suitable approach, as it is cost-effective, simple to operate, and sensitive in removing toxic and polluting substances (Mashkoor & Nasar, 2020).

Nanocellulose is a cellulose substance that has been treated down to the nanoscale (Dufresne, 2019). Nanocellulose is a promising nanomaterial derived from cellulose with numerous potential applications in fields such as electronics, sensors, and energy storage. However, a key limitation of nanocellulose is its inherent lack of intrinsic magnetic properties. The absence of magnetic functionality in nanocellulose restricts its use in certain applications that require materials with the ability to interact with magnetic fields. This poses a challenge to fully leverage the unique structural, mechanical, and biocompatible properties of nanocellulose in a wider range of technological innovations. Developing strategies to impart magnetic behavior to nanocellulose, without compromising its other desirable characteristics, is an important research objective. Potential approaches to addressing this problem may involve the incorporation of magnetic nanoparticles or the chemical modification of nanocellulose to induce permanent or induced magnetism. The magnetic properties of magnetite-impregnated nanocellulose allow for easy separation and recovery of the dye-laden material using an external magnetic field, reducing the time and cost associated with traditional filtration or centrifugation methods. By developing magnetite-impregnated nanocellulose as an effective adsorbent for methylene blue dye, aim to address the challenge of efficient dye removal and recovery, ultimately contributing to the development of sustainable and environmentally friendly wastewater treatment technologies (Hokkanen & Sillanpää, 2020).

1.3. Objectives

1.3.1. General Objective

The main objective of this study was removing MB from an aqueous solution using magnetite impregnated khat stem based nanocellulose composite.

1.3.2. Specific Objectives

- To synthesis nanocellulose derived from the khat stem extracted cellulose suspension.
- To synthesize magnetite impregnated nanocellulose composites.
- To characterize the prepared cellulose, nanocellulose, and magnetite impregnated nanocellulose composite by using FTIR, DSC, SEM, BET, and XRD techniques.
- To investigate MB dye removal efficiency of the MNC composite adsorbent.
- To investigate the adsorption isotherm and kinetics.
- To investigate the reusability of MNC.

1.4. Significance of the Study

The core significance of this thesis work lies that use of a low-cost adsorbent facilitated the removal of methylene blue (MB) dye from aqueous solutions, thereby contributing to the production of clean water and the betterment of the overall environment. Also, khat stem and related wastes are becoming an environmental burden in urban areas as these wastes are disposed of on the roadside and drainage lines. In order to reduce this burden, this study could play a significant role by converting the khat stem into nanocellulose and MNC, which can be used for the adsorption of dye pollutants from an aquatic system.

1.5. The Scope of the Study

This thesis work was done on an aqueous solution that contains MB dyes prepared at the ASTU laboratory. The khat stems were collected from Adama Town. This study investigated the use of nanocellulose from the khat stem and it's impregnated with magnetite nanocomposites as an adsorbent for the removal of methylene blue (MB) dyes from aqueous solutions. Adsorbent was characterized using X-ray diffraction, DSC, FTIR, SEM, BET, and UV-visible spectroscopy.

CHAPTER TWO

2. LITERATURE REVIEW

2.1. Water Pollution

The distant past of human control and utilization of freshwater resources is intimately associated with the growth of human civilization (Bănăduc et al., 2022). Every living thing depends on water, but unfortunately, industrialization and increased urbanization have a negative effect on clean water sources (Hassan Rashid et al., 2018). Numerous things have the potential to pollute water. Either people and animals are at risk due to these harmful substances, which include toxic metals, surfactants, insecticides, herbicides, dyes, and chlorophenols (Rathi et al., 2021). Numerous health hazards, such as irritation of the skin, eyes, respiratory system, sore throat, and asthma, can result from exposure to organic dyes (Chung, 2016).

Dyes are colorful substances designed to give materials such as fabrics, papers, or any colorable materials a hue (Abd-Elhamid et al., 2020). The colorful aromatic chemical molecules identified as dye are what give objects that are visible their color by absorbing light region. different dyes are employed for numerous reasons in a broad range of industries, such as the food, paper, plastic, cosmetic, and pharmaceutical (VTD Alencar et al., 2020). These companies produce huge quantities of wastewater that pollute water with hazardous and carcinogenic dyes, unsafe intended towards use by humans (Pandey et al., 2020). Textile dyes are exceptionally complex substances that have several structural groups used in the textile industry. more than any other industry (Fong et al., 2020). MB is one among the dyes usually used to color silk, wool, cotton, and pulps trade (Derakhshan et al., 2013).

2.1.1. Methylene Blue Dye

Dyes can be classified into cationic and anionic dyes. Anionic dyes depend on a negative ion. Anionic dyes includes many compounds from the most varied classes of dyes, which exhibit characteristic differences in structure (e.g., azoic, anthraquinone, triphenylmethan and nitro dyes) but possess as a common feature, water-solubilizing, ionic substituents. The anionic dyes also include direct dyes, and from the chemical standpoint the group of anionic azo dyes includes a large proportion of the reactive dyes (Amran et al., 2011). Cationic dyes are widely used in acrylic, wool, nylon and silk dyeing. These dyes include different chemical structures based on substituted aromatic groups. This group of dyes is considered as toxic colorants and can cause harmful effects such as allergic dermatitis, skin irritation, mutations and cancer (Tripathi, 2019).

Cationic dyes carry a positive charge in their molecule, furthermore it is water soluble and yield colored cations in solution. Cationic functionality is found in various types of dyes, mainly in cationic azo dyes and methane dyes, also in anthraquinone, di- and tri-arylcarbenium, phthalocyanine dyes, various polycarbocyclic and solvent dyes. The anthraquinone dyes are expensive and weak while the azo dyes have good properties, strong thus reducing cost (Amran et al., 2011). Cationic dyes were used intensely as a model in dye adsorption studies such as Crystal violet, Methylene blue, Basic blue 41 and Basic red 46 (Amran et al., 2011). Methylene blue is an important basic dye and widely used in the textile industry. Methylene blue dye is a solid green powder at room temperature. When it's mixed with water, it forms a blue solution (Chakraborty et al., 2016).

MB exhibits solubility in methanol, 2-propanol, water, ethanol, and acetone and ethyl acetate (Salimi & Roosta, 2019). At 25°C, it dissolves in water at an amount of 43.6 g/L (Pham et al., 2020). Since practically all calculations in photo degradation and adsorption investigations rely on the material's UV-visible spectra, UV analysis of MB is critical. The strongest absorption peak in the MB absorption spectra the spectrum exhibits two main peaks, a peak around 664 nanometers (nm) corresponds to a single molecule (monomer) of the Methylene Blue (MB) dye. A secondary peak, located at about 612 nm, is associated with MB molecules paired together (dimer). Additionally, in the ultraviolet (UV) region, two more bands are observed with peaks at 292 nm and 245 nm. These UV bands are likely linked to aromatic ring structures containing a single carbon atom substitution (substituted benzene rings (Mondal et al., 2017).

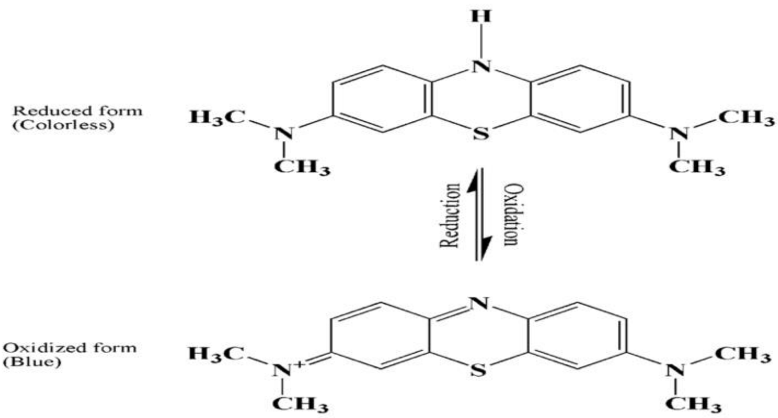

Figure 1: Structure of methylene blue

2.1.2. Application of Methylene Blue

MB dye has many potential applications in the textile, pharmaceutical, paper, dyeing, printing, paint, medicine, and food industries. It is the most common dye in the textile industry, and is considered one of the most popular clothing colorants. MB firmly adheres in the interstitial spaces of cotton fibers and is fixed firmly on fabric in the textile industry (Khan et al., 2022). MB is used to estimate rock swelling, which is used as a quick test to assess the quality of foundry sand in foundries. MB dye is also used as a photosensitizer, an oxidation-reduction indicator, an optical redox indicator in analytical chemistry and in the trace analysis of anionic surfactants. It is also used as a potential material in dye-sensitized solar cells, capacitors, sensors, microbial fuel cells, etc. (Khan et al., 2022).

MB is a versatile molecule with a range of properties that make it valuable in biological applications. Historical significance as synthetic antimalarial used against all forms of the disease in the late 19th and early 20th centuries, MB also serves as effective medicinal drug treating conditions like Barrett's esophagus and anemia. Furthermore, MB possesses the additional ability to sensitize the body to chloroquine (Shi et al., 2018; Schirmer et al., 2003). Methylene blue dye is employed in the treatment of cancer through photodynamic therapy (M. K. Uddin & Nasar, 2020). It is widely employed to photosensitize plasma for the treatment of photodynamically inactivating RNA viruses, including hepatitis B, HIV, and hepatitis C (Saha et al., 2018). From current studies, MB could enhance memories and prevent Alzheimer's disease (Ye et al., 2024).

2.1.3. Toxicity of MB Dye

Dyes are widely used in various industries, such as textile, paper, plastics, and cosmetics, which can lead to their release into the environment. The presence of dyes in water bodies can be detrimental to aquatic ecosystems, as they can reduce light penetration and affect photosynthesis, ultimately disrupting the food chain (Gayathri et al., 2015). Additionally, many dyes, including methylene blue, are known to be toxic and can have adverse effects on the health of living organisms. Methylene blue is a synthetic dye commonly used in various applications, including as a coloring agent, a medication, and a redox indicator. However, the improper disposal of methylene blue-containing wastewater can pose significant environmental and health risks. Exposure to methylene blue can cause skin irritation, eye irritation, and respiratory problems in humans, and it has also been linked to more severe health issues, such as cardiovascular and neurological problems (Abdelrahman et al., 2019).

In addition, it results in accelerated heart rate, methemoglobinemia, tissue necrosis, nausea, vomiting, diarrhea, cyanosis, shock, gastritis, jaundice, and premature cell death in tissues (Khan et al., 2022). Furthermore, methylene blue is a persistent pollutant that is not easily degraded in the environment. It can accumulate in soil and sediments, leading to long-term contamination and potential bioaccumulation in the food chain (Ebi Ebi et al., 2018). The presence of methylene blue in water bodies can also interfere with the treatment of drinking water, making it a concern for public health. Its enormous molar absorption coefficient (~8.4 × 104 L mol^{-1} cm^{-1} at 664 nm) affects the biological community's diversity and attractiveness, sunlight transmittance, oxygen solubility, and aquatic life's ability to photosynthesis (Khan et al., 2022).

2.2. Nanocellulose (NC)

Plant fibers are mostly made of cellulose, which considered the most abundant natural polymer and is responsible for providing rigidity to plants. Humans have utilized cellulose, for a variety of building applications. It is mostly utilized as paper and board, undamaged wood, and textile fibers like cotton and flax (Olsson & Westm, 2013). Additionally, cellulose provides a flexible platform for a variety of chemical processes (Klemm et al., 2005). Cellulose is the common polysaccharide by nature and a higher substitute for a number of products since it is a nontoxic, biodegradable, and chemically stable polymer

(Jonoobi et al., 2015). Cellulose is a linear biopolymer made up of β-D-glucopyranose units that are connected by β-glucosidic bonds (β 1–4), with intramolecular interactions taking place between the adjacent cellulose units. Three hydroxyl groups and six carbons make up each glucose unit. These units can create fibril cellulose, which is composed of both amorphous and crystalline areas, cellulose chains, and supramolecular cellulose layers constructed by crystalline cellulose (Olsson & Westm, 2013; Roa et al., 2021). The structural chain of cellulose will be presented in Figure 2.

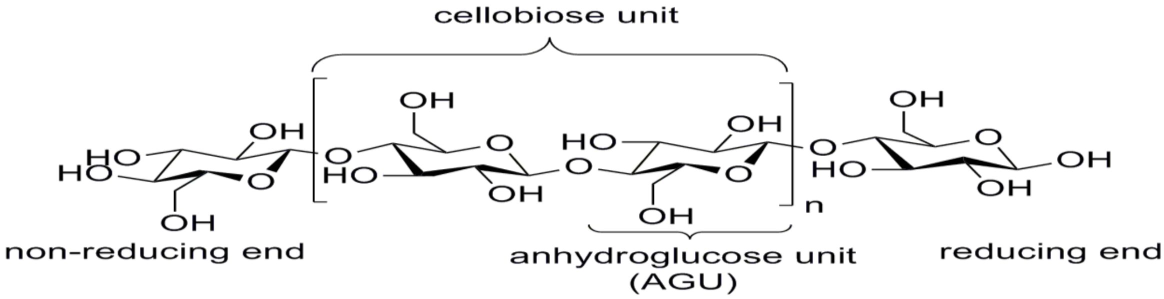

Figure 2: The cellulose polymer structural chain.

Nanocellulose is gaining popularity in the area of nanotechnology due to its effectiveness and energy efficiency. Nanocellulose's advantages make it a popular choice for large-scale production. It serves as a building block for crucial components in various industries, including food, paints, textiles, and pharmaceuticals (Mishra et al., 2018). Nanocelluloses are classified into two types:, cellulose nanofibrils and cellulose nanocrystals (CNCs), sometimes referred to as nanocrystalline cellulose and cellulose nanowhiskers sometimes called nano-fibrillated cellulose (Omran et al., 2021).

In addition to their larger surface area, biocompatibility, and reactive OH group in the surface CNCs are suited for varies advanced functional applications, including tissue engineering, medication administration, strengthening of materials, waste water treatment, and others qualities (Jorfi & Foster, 2015). The high density of hydroxyl groups in cellulose molecules makes them less soluble in water, but these linkages also facilitate the formation of cross-linked hydrogen networks. The adsorbent activity is related to this type of impact. improve removal of specific contaminants, the hydroxyl groups of cellulose can be replaced with specific functional groups, such as carboxyl, sulfonic, and cyclodextrin groups (Cova et al., 2021). Cellulose can be derived from a diverse range of sources, including trees, annual plants, microbes, and animals (Jonoobi et al., 2015).

2.2.1. Khat Stem as Source of cellulose

The Middle East and the Horn of Africa are home to the evergreen shrub known as "khat," or Catha edulis Forsk. Catha edulis, the plant commonly referred to as khat, is found all throughout the African horn, and people chew its leaves to get high (Olani et al., 2023). Khat is a plant that was mostly grown in Ethiopia and Yemen until recently, where it continued to grow for a very long period (Gebissa, 2010). But in recent years, cultivation of it has begun, spreading to most of eastern Africa, as well as to Madagascar, South Africa, and Afghanistan in the west (Getasetegn, 2016).

Due to its euphoric and psychostimulant effects, millions of people chew fresh leaves of khat plant every day as a recreational drug (Nichols et al., 2015). Ethiopia is the leading global producer of the khat, which is currently the commodity with the quickest rate of growth for exports (Rameshwar & Argaw, 2016). For many years, people from various walks of life used khat, including kids, expectant mothers, pregnant women, and those taking medication (Bedada et al., 2018). Because of economic attractiveness, khat cultivation by local farmers is extending with a rapid decreasing in annual crop production (Gessesse Dessie, 2013). On more than 250,000 hectares of land, more than two million farmers grow khat (Wuletaw, 2018).

Older leaves and branches from the khat plant are disposed of as solid garbage after the young leaves are harvested for chewing locally and exported. Cities and towns with significant amounts of solid khat waste have lost part of their aesthetic appeal and have turned into havens for certain rodents and vectors. Additionally, the garbage encourages some people to dispose of more, which exacerbate the cities' and towns' poor sanitation. Due to the massive amount of trash produced, appropriate disposal methods are required (Rameshwar & Argaw, 2016). Such waste material could be turned into valuable products like cellulose and its derivatives, which would address a number of socioeconomic issues and provide a more environmentally friendly way to use waste by addressing ecological and economic cases like avoiding deforestation and environmental pollution.

Chemists used early, fascinating research on the khat plant to identify the primary psychotropic component, cathinone (Lo Faro et al., 2020). This plant's leaves and roots contain a wide variety of compounds that fall into different chemical classes. These include cathedulins, flavonoids, sterols, triterpenes, monoterpenes, volatile aromatic compounds also, the alkaloids of phenylalkylamines (Aklillu & Engidawork, 2021). The chemical composition of untreated khat waste (KW) is cellulose (39.4 ± 0.38), hemicellulose (12.75 ± 0.52), and Klason lignin (28.67 ± 2.46) (Gabriel et al., 2021). Untreated khat can be treated in a variety of ways, increasing the amount of cellulose. Khat's cellulose content can reach 88% after treatment with formic and acetic acids (Gabriel et al., 2021).

2.3. Pretreatment Method of Cellulose

Extraction of cellulose may involve many methods based on the biomass source, production type, and anticipated cellulose grade (Brinchi et al., 2013). Various methods for extracting cellulose have been actively explored, with some of them patented. However, the majority of the technologies have three primary processes: biomass conditioning, pretreatment to remove lignin and hemicellulose, and purification or bleaching to remove remaining lignin and hemicellulose (Abolore et al., 2024). Biomass conditioning consists of washing to remove dirt and pigment matter, size reduction, refluxing with ethanol and deionized water to remove extractives, drying, and sifting (Abolore et al., 2024). The advantages of biomass pretreatment include the disruption of the lignin structure and the increase in available surface area for subsequent chemical, microbial, and enzymatic processes. Following biomass pretreatment, the dried biomass is often subjected to further processing to solubilize the lignin and hemicellulose components, with the goal of isolating the cellulose fibers.

Acid-based and alkaline-based pulping are the most common biomass pretreatment methods employed for this purpose. Subsequently, the cellulose is bleached to remove the colored lignin and degraded chemicals remaining from the cellulosic material. This bleaching process involves the oxidation of the water-insoluble lignin using bleaching agents like hypochlorite and peroxide, which breaks specific bonds and generates water-soluble molecules such as aromatic aldehydes and carboxylic acid (T. Wang & Zhao, 2021). Bleaching chemicals accelerate the removal of lignin and hemicellulose is achieved by disrupting the linkages between these components. To ensure complete elimination of all binding agents, the bleaching process is typically repeated multiple times until white cellulose fibers are produced, indicating the successful completion of the bleaching.

Additionally, recent research has focused on the delignification of lignocellulosic materials using a combination of low-boiling carboxylic acids, such as formic and acetic acids, along with water (Demesa et al., 2020). It has been stated this method utilizing low-boiling carboxylic acids and water can operate at relatively low temperatures under atmospheric pressure conditions.

Additionally, the solvents involved can be recycled, and the extracted lignin and hemicelluloses can be recovered for various applications. The hemicelluloses produced through this approach have been employed for biofuel generation and animal feed, while the lignin extracted using the formic acid/acetic acid/water mixtures has demonstrated promising applications in the manufacture of phenoplast and aminoplast resins, adhesives, and polyurethane products (Assonfack et al., 2023). The combination of formic acid and acetic acid for cellulose pretreatment can be beneficial. Formic acid and acetic acid have distinct mechanisms of action. Formic acid dissolves hemicellulose and lignin, whereas acetic acid increases accessibility and selectively dissolves hemicelluloses. When used simultaneously, they can enhance delignification and cellulose accessibility. Acetic acid is useful in the removal of lignin, although formic acid alone may not be sufficient. The combination can result in enhanced delignification (Huang et al., 2020). While formic acid recovery can be costly, combining acids allows for lower concentrations of each, potentially lowering overall costs.

2.4. Methodologies for the Synthesis of nanocellulose

Plants, agricultural waste, and other materials having a high proportion of cellulose are utilized valuable materials in a huge of applications because their low cost, environmental friendliness, biodegradability, and other beneficial features (Daifullah et al., 2003). Nanocellulose isolated by different ways, such as: enzymatic, mechanical, chemical, and physicochemical procedures (Thomas et al., 2019). Before selecting a certain extraction method, several critical characteristics are considered, including the material's surface area, porosity, crystallinity, and chain length (Phanthong et al., 2018).

2.4.1. Chemical methods of isolation

Alkaline pretreatment, involves use of alkaline chemicals to disrupt lignocellulosic structure and increase the accessibility of cellulose. separation techniques are among the chemical techniques used to separate nanocellulose from nanocellulosic materials (Thakur et al., 2021). The alkaline technique to delignification necessitates a pre-treatment with alkalis like, NaOH, KOH, $Ca(OH)_2$, NH_3 and Na_2CO_3 (J. S. Kim et al., 2016). This approach allows the alkali reagent to be easily retrieved once the reaction is completed at a significantly lower temperature and pressure. However, it has substantial disadvantages in the isolation process due to the requirement for highly concentrated alkaline reagents and the extended reaction time (Sarkar et al., 2012).

On the other hand, the acid method uses concentrated and diluted acids, like HCl (H. Wang et al., 2010), H_3PO_4 (Y. P. Zhang et al., 2007), for the isolation of nanocellulose. Because concentrated acids are dangerous and corrosive, the acid technique has a major disadvantage (Li & Knierim, 2010). The extraction of nanocellulose is also accomplished by solvent extraction pretreatment, which involves the application of several solvents, such as ethers, ketones, benzene (C_6H_6), triethylene glycol ($C_6H_{14}O_4$), butanol (C_4H_9OH), methanol (MeOH), ethanol (EtOH), and so on (Tixier et al., 2003). The expensive cost of organic solvents, the need for an instrument setup, and the volatile organic solvents limit the pretreatment method's demand for industrial applications are some of its primary disadvantages (Ko et al., 2009).

2.4.2. Enzymatic methods of isolation

Nanostructured cellulose is produced by pretreating bleached cellulose using an enzyme process. A combination of celluloses is needed to break down cellulose; hence it cannot be done with only one type of enzyme ($C_{18}H_{32}O_{16}$) to disintegrate cellulose (($C_6H_{10}O_5$)n). Compared to alternative chemical methods, the enzymatic pretreatment offers significant benefits like higher yields, environmental friendliness, increased selectivity, lower energy costs, and softer reaction conditions (S. Sun et al., 2016). The two main disadvantages of this approach, according to Pedersen and Meyer, are the elevated cost of enzymes and the extended processing time necessitated for cellulose disintegration pose challenges (Weiss et al., 2013).

2.4.3. Mechanical methods of isolation

Pretreatment using mechanical means High pressure homogenization, sonication, and cryocrushing techniques are some of the isolating processes utilized to produce fine fibers (Jonoobi et al., 2015). With the high pressure homogenization approach, nanocellulose can be effectively isolated without being treated with hazardous organic solvents (Thakur et al., 2021). Sugarcane bagasse was isolated using high pressure homogenization pretreatment, as demonstrated by wang et al (Y. Wang et al., 2017).

2.4.4. Physicochemical methods of isolation

The natural fibers undergo a two-step pretreatment process. First, they are chemically pretreated, likely using one of the methods mentioned previously, such as alkaline, acid, or oxidation-based treatments. Then, the chemically pretreated fibers are mechanically processed using techniques like sonication or homogenization. techniques in the physicochemical way, which combines the chemical and mechanical procedures (Brodeur et al., 2011). According to Wang and Sain, CNFs were isolated from a soybean source via chemo-mechanical treatment, in which the cellulosic material first undergoes chemical processing before being subjected to mechanical processing (refining and pounding) (B. Wang & Sain, 2007).

2.5. Iron Oxide Nanoparticles

The second-most common element on Earth is iron. Magnetite (Fe_3O_4), also known as ferrous ferric oxide, is one of the two main types of iron oxide. It is widely used in many different applications and exhibits superparamagnetic properties. The oxidized form of magnetite is called maghemite (γ-Fe_3O_4) (Baabu et al., 2022). Applications for iron oxide nanoparticles include targeted drug administration, magnetic particle imaging, and biomedical imaging. Chemical processes are catalyzed by iron oxide nanoparticles. In terabit magnetic storage devices, they have a function. They cause localized hyperthermia, which is utilized as a cancer treatment. Biomolecules can be separated by iron oxide nanoparticles. They are investigated for contaminant removal and water purification. Additionally, dietary supplements have been made with iron oxide nanoparticles (Ali et al., 2016).

2.5.1. Magnetite Nanoparticles

Magnetite, a prevalent magnetic iron oxide, has a cubic inverse spinel crystalline structure, where iron cations are situated in both tetrahedral and octahedral positions, and the oxygen atoms form a face-centered cubic close packed lattice (Darcheville, 2021). Magnetite has been widely employed in variety of industries, including water purification, chemical production, pharmaceutical applications, and magnetic separation and storage (El-Gendy & Nassar, 2021). Magnetite nanoparticles are very desirable for a variety of applications because of their nanoscale size, well defined surface form, and natural magnetic properties (Wallyn et al., 2019). There are different methods to synthesis magnetite. A common technique for creating magnetite (Fe_3O_4) nanoparticles is coprecipitation. Under extremely basic circumstances, ferric (Fe^{3+}) and ferrous (Fe^{2+}) ions precipitate from a solution simultaneously in coprecipitation (John, 2017). Iron ion hydroxides that precipitate combine to generate magnetite nanoparticles. Numerous benefits occur with the coprecipitation technique. Because of its large yield of nanoparticles, it can be manufactured on an industrial range. This process also simple and isn't necessary for a lot of sophisticated apparatus or extremely hot temperatures. Because common chemicals are used, it is an inexpensive method. Coprecipitation minimizes the impact on the environment because it happens in mild conditions (Yıldız et al., 2016).

2.6. Magnetite Nanocellulose

Magnetite (Fe_3O_4) nanoparticles have recently attracted scientists' attention due to their exceptional performance, which includes ability to exhibit superparamagnetic behavior with high saturation magnetization when an external magnetic field is applied, as well as their small size, good biocompatibility, low toxicity, and favorable physicochemical stability (Xu & Lee, 2021). Nanocellulose combined with magnetite has unique magnetic characteristics. This means that the material can be attracted to or repelled by an external magnetic field, allowing for simple manipulation and separation in magnetic fields (Sriplai & Pinitsoontorn, 2021). Because of its magnetic properties, this material is versatile for a varieties applications, including environmental cleanup, medical engineering, and also electronics (Kumar et al., 2021). Also, very useful for applications like magnetic separation of pollutants from water or tailored medication administration in medical applications (Kumar et al., 2021). The magnetic characteristics of nanocellulose coated with magnetite result in rise surface area and adsorption capacity. Presence of magnetite nanoparticles allows the composite to effectively capture and retain target molecules or pollutants (Y. Zhao et al., 2020). It also allows the material to be easily retrieved and reused during adsorption studies. Separating the composite from solution using external magnetic field allows for rapid regeneration and several cycles of use. This reusability property enhances the material's sustainability and economic effectiveness in a variety of applications (Hokkanen & Sillanpää, 2020).

2.7. Dye removal techniques

As industrialization progresses, the detrimental effects of various enterprises' effluent emissions represent a serious threat to a range of life forms, pollutants must be removed before wastewater is released into the environment due to its enormous environmental impact and increased public awareness of environmental protection issues. There are currently several ways available for removing colors from industrial effluents. However, not all treatments are equally effective, and each has limitations due to the wide range of colors available and the complexity of the effluent. Treatment procedures are generally grouped three distinct categories: chemical, biological, and physical (Yuan et al., 2019). The common advantage and disadvantage of conventional and advanced techniques are list in table 1.

Table 1: Advantages and disadvantage of different dye removal techniques

Methods	Advantages	Disadvantages	Reference
Advanced oxidation process	Proficiently degrades the dyes at ambient pressure and temperature, organic pollutants are oxidized to carbon dioxide	High maintenance and operation cost, not flexible	(Gupta & Suhas, 2009)
Chemical precipitation	Simple, inexpensive, handle high contaminant loads, easiness in handling, integrated physio-chemical process, a substantial decrease in COD	Involves large numbers of chemicals, excessive sludge generation	(Crini & Lichtfouse, 2019)
Ion exchange	No sludge generation, consume less time, produce high quality water, effective decolorization technique.	Performance is highly pH-sensitive, not effective for all dyes, expensive in recharging and generation of large sludge	(Crini & Lichtfouse, 2019)
Electrochemical method	Chemicals are either not required or at least minimized, fast process, suitable for insoluble and soluble dye with the lessening of COD	high maintenance charges, high electricity cost, sludge generation and also pollution from heavy metals and chlorinated organics owing to indirect oxidation	(Gupta & Suhas, 2009)
Oxidation	Complete degradation of dyes,	Maintenance of pH,	(Holkar et

	reaction time is short	catalyst require for effective treatment, expensive	al., 2016)
Ozonation	Fast, effective disinfection, easy installation of equipment	Short half-lifetime, expensive method, generation of noxious intermediates and by-products, careful pH maintenance of the effluent	(Collivignarelli et al., 2019)
Biological methods (aerobic and anaerobic)	The cost-effective, eco-friendly, non-hazardous end product and complete mineralization	Less biodegradability of the dyes, highly depends on reaction conditions, inflexibility in design and operation, the requirement of large land area, requisite of longer time for decolorization	(Holkar et al., 2016)
Coagulation and flocculation	Most widely used physiochemical method for dyes removal, coagulating agent remove completely from the treated wastewater, effective, easy operation, complete decolorization	Recycling of costly chemicals is not viable, not suitable for highly water-soluble dyes, generation of colored coagulated solid waste, production of toxic sludge, increase in TDS in treated wastewater, not an Environmentally sustainable technique	(Singh & Arora, 2011)
Adsorption	Simple, highly effective, easy and wide applicability, the admirable capability to remove an extensive range of contaminants, economic, adsorbents may be prepared from wastes, the possibility of adsorbent regeneration	Efficacy rely on the nature of adsorbents, chemical modification of adsorbent is required to improve their adsorption capacity, some adsorbents are very costly	(Collivignarelli et al., 2019)

2.7.1. Adsorption

Adsorption, which is a surface-based process, adsorbate molecules or ions whether from a liquid or gas phase, accumulate and concentrate on the surface of a solid material.

Adsorption is the process by which molecules or particles adhere to and accumulate on the external surface of a solid material, or its internal surface if the substance is porous, in a thin layer. Adsorbents are solid materials that adsorb a pollutant or target substance, while the target substance is also known as an adsorbate. The adsorption of dye molecules onto the surface of an adsorbent can occur through a range of forces, such as hydrogen bonding, electrostatic interactions, van der Waals forces, hydrophobic interactions, and others. Adsorption processes are generally divided into two types: physisorption and chemisorption (Berger & Bhown, 2011).

Adsorption is a highly effective and versatile technique for the removal of methylene blue dye from aqueous environments. One of the primary advantages of adsorption is the high adsorption capacity that can be achieved, with studies reporting capacities ranging from 100 to 500 mg/g for various adsorbent materials (Hameed et al., 2007). Additionally, the adsorption process exhibits rapid kinetics, allowing for efficient dye removal within a short contact time, typically less than an hour (Gao et al., 2013). Another notable benefit is the ease of separation and recovery of the dye-laden adsorbent, which can be facilitated through the use of magnetic or gravitational separation methods. This simplifies the post-adsorption treatment and enables the potential reuse and regeneration of the adsorbent material, promoting sustainability and cost-effectiveness (Jodeh et al., 2018).

Furthermore, adsorption-based techniques are generally environmentally friendly, as they can utilize renewable and biodegradable materials, aligning with the principles of green chemistry and sustainable waste management. The adsorption process presents an attractive and effective alternative approach for the removal of dyes from wastewater (R. Rashid et al., 2021). The key factors that govern the performance of most adsorption processes are typically the initial dye concentration, solution pH, temperature, contact time, and adsorbent dosage. Optimization of these conditions is crucial for the development of an effective industrial-scale dye removal treatment process. The following discusses some of the key factors affecting the adsorption of dyes.

1. Effect of solution pH

The pH of the solution is a crucial factor in determining the adsorbent's ability to remove dye. The adsorption efficiency is dependent on the solution pH, as changes in pH can alter the degree of ionization of the adsorbate molecule as well as the surface properties of the adsorbent (Yagub et al., 2014). The interaction between the adsorbent and adsorbate is governed by the surface charge of the adsorbent, which is in turn determined by the pH level of the solution. The impact of pH on dye adsorption by any adsorbent can be attributed to two potential mechanisms; the electrostatic interaction between the protonated or deprotonated groups of the adsorbent and the dye molecules, as well as the chemical reaction between the adsorbate and the adsorbent. The adsorption of other ions is affected by the solution pH, because the hydrogen and hydroxyl ions tend to be adsorbed more quickly. Adsorptive process is impacted by pH variation because they cause functional groups of the adsorbent's active sites to dissociate. Therefore, the equilibrium properties of adsorption process and the reaction kinetics change. It is a well-known fact that surface actively attract cations at a higher pH levels because of deposition of OH^- ions, but it also positively adsorbs anions at lower pH levels because of presence of H^+ ions (Yagub et al., 2014).

2. Effect of adsorbent dose

The adsorbent dosage is a critical process parameter for determining the capacity of an adsorbent for a given amount under the specified operating conditions. In general, the removal effectiveness increases with higher adsorbent dosage, as the number of sorption sites on the adsorbent's surface grows proportionally with the amount of adsorbent used. The effect of adsorbent dosage provides insight into the ability of dye sorption to be absorbed using the minimum amount of adsorbent, allowing one to recognize the capacity of the adsorbent from an economic perspective (Sartape et al., 2017).

3. Effect of Interaction time

The time pollutants spend in contact with the adsorbent material (contact time) is crucial for wastewater treatment using adsorption. Effective adsorbent materials quickly capture pollutants and reach a state of balance (equilibrium) within a short timeframe. This is especially true for physical adsorption, where most pollutants attach to the adsorbent surface relatively quickly. However, if there's a strong chemical attraction For the system to reach a stable state (equilibrium) where pollutant capture is balanced, a longer contact time might be required, especially when there's a strong attraction between the pollutant and the adsorbent material. Initially, the rate of pollutant capture appears steady because there are many empty spaces (vacant surface sites) on the adsorbent for pollutants to attach to. However, over time, these empty spaces become harder to fill due to repulsive forces between the captured pollutant molecules on the adsorbent's surface and the remaining pollutants in the water (bulk phase) (Nasr et al., 2017).

4. Dye concentration

The amount of dye present at the start (initial dye concentration) strongly influences how much dye needs to be captured (adsorbed) for removal. This is because there's a direct link between the dye concentration and the number of "parking spaces" (adsorption sites) available on the adsorbent's surface. Generally, as the initial dye concentration increases, the percentage of dye removed decreases. This likely happens because the "parking spaces" on the adsorbent get filled up (saturated). Interestingly though, a higher initial dye concentration can also lead to the adsorbent grabbing more dye overall (increased capacity). This might be because there's more "dye traffic" (mass transfer driving force) pushing the dye towards the adsorbent when there's a lot of dye present initially (Yagub et al., 2014).

2.7.2. Dye Adsorption by NC and MNC

Dyes are a type of contaminant that is commonly employed in the textile industry and can be detected by the human eye. Their applications include tannery, medicines, paper, paints, plastics, and cosmetics (VTD Alencar et al., 2020). For a variety of reasons, nanocellulose is the best adsorbent. It is made from cellulose, the most prevalent organic biopolymer on Earth. It can be generated from numerous renewable materials such as wood, plants, or agricultural waste, making it a cost-effective adsorbent material (Kanmani et al., 2017). It possesses a huge specific surface area due to its nanoscale size, which boosts its adsorption capability (Voisin et al., 2017). Nanocellulose surfaces are intrinsically hydrophilic, allowing them to interact with polar adsorbates the chemically and mechanically pretreated natural fibers can then be utilized for the adsorption and removal of various pollutants, such as heavy metal ions and dyes. The hydrophilic nature of the cellulose fibers resulting from the pretreatment process improves their adsorption capacity towards these types of contaminants capacity and selectivity. Nanocellulose is also biodegradable and does not produce hazardous byproducts during its life cycle (Peter et al., 2022).

The adsorption kinetics using the pretreated natural fibers were found to be rapid, with equilibrium typically achieved within 1-2 minutes of contact time. For example, cellulose nanofibers (CNF) prepared from kenaf core using an acidified chlorite bleaching method, followed by high-speed blender disintegration, were effective in adsorbing methylene blue, a cationic dye. The study investigated the effects of disintegration time and acid treatment on the defibrillation of the holocellulose. The maximum adsorption capacity was around 123 mg/g, achieved at a temperature of 200°C and pH 9. In this case, just 1 minute of contact time was sufficient to reach equilibrium.

Furthermore, the CNF adsorbent could be regenerated by treatment in an acidic medium. However, the adsorbent was observed to be exhausted after six cycles of adsorption-desorption (Chan et al., 2015). Compared to the previous study using cellulose nanofibers (CNF), a similar investigation utilized cellulose nanocrystals (CNCs) prepared via sulfuric acid hydrolysis of cellulose fibers as the adsorbent for methylene blue (MB) removal from aqueous solutions. The adsorption equilibrium data for the CNC adsorbent was found to fit both the Langmuir and Freundlich isotherm models. The maximum adsorption capacity achieved with the CNC adsorbent was 118 mg/g at 25°C and pH 9. Interestingly, when the CNCs were further modified via TEMPO-oxidation, the adsorption capacity increased significantly to 769 mg/g CNC (Batmaz et al., 2014).

Magnetite nanocellulose (MNC) is a promising adsorbent material that has gained significant attention in recent years due to its excellent adsorption capacity, ease of separation, and environmentally friendly nature. The adsorption of MB by MNC involves the interaction between the dye molecules and the surface of the MNC, which is influenced by various factors such as pH, temperature, contact time, and initial dye concentration. Several studies have been conducted to investigate the adsorption of MB by MNC. For example, a study by Jodeh et al., (2018) reported that MNC exhibits a high adsorption capacity for MB, with a maximum adsorption capacity of 196 mg/g. The authors attributed the high adsorption capacity to the synergistic effect of the cellulose and magnetite components, which provide a large surface area and magnetic properties for efficient separation.

Another study by Melhem, (2017) explored the kinetics and thermodynamics of MB adsorption on MNC. The results showed that the adsorption process followed a pseudo second order kinetic model and was endothermic in nature, indicating that the adsorption was spontaneous and favorable at higher temperatures, and also Langmuir adsorption isotherm was more fit than the Freundlich model. Furthermore, X. Sun et al., (2022) investigated the effect of surface modification of MNC on the adsorption of MB. The authors found that the modification of MNC with polyethyleneimine (PEI) significantly improved the adsorption capacity and used for the adsorption of heavy metals and dyes. In conclusion, magnetite nanocellulose is a promising adsorbent material for the removal of methylene blue dye from wastewater. The adsorption process is influenced by various factors, and the high adsorption capacity of MNC can be attributed to its unique properties and the potential for surface modification. Further research is needed to optimize the adsorption process and explore the potential applications of MNC in real-world wastewater treatment scenarios.

C HAPTER THREE

3. MATERIALS AND METHODS

3.1. Materials

3.1.1. Equipment and Instruments

The following equipment and instruments were used to perform the study. Different size beakers, micropipettes, stirrer, volumetric flasks, funnels, measuring cylinders, test tubes, thermometers, refrigerator, stopwatches, ovens, plastic bags, different sizes Erlenmeyer flasks, filter papers, shaker, source materials (khat stem), aluminum foil, cuvette, electrical balance, XRD (Shimadzu XRD-7000), FTIR, DSC, SEM, BET, UV-Vis spectroscopy, pH meter, centrifuge and scissors.

3.1.2. Chemicals and Reagents

The study was conducted using analytical graded chemicals and reagents. Hydrogen peroxide (30%, Fine Chemical Central Trading) was used to bleach the cellulose. Solution of sodium hydroxide (99%, LABKEmical) and hydrochloric acid (35-38%, Alpha chemika) were used for adjustment of pH, and distilled water (DW) used to prepare stock solution; tap water was also used to wash the khat stem, and sulfuric acid (98%, LOBAL Chemie Laboratory reagent and fine chemicals) was used for nanocellulose synthesis. Formic acid (98%, Sisco Research Laboratory Pvt. Ltd.), and acetic acid (99.5%, LOBAL Chemie laboratory reagent and fine chemicals) were also used for cellulose extraction. Methylene Blue Trihydrate, $C_{16}H_{18}C_lN_3S \cdot 3H_2O$ (99%, (Samir Tech-Chem, PVT, LTD) was selected to prepare a representative dye pollutant. The sources of iron used to create MNC and magnetite nanoparticles were $FeCl_2.4H_2O$ (99%, Sigma-Aldrich) and $FeCl_3.6H_2O$ (97%, Sigma-Aldrich). MNCs and magnetite nanoparticles were washed using ethanol (96%, Fine Chemical Central Trading).

3.2. Methods

3.2.1. Cellulose Extraction

The khat wastes (KWs) were collected from Ethiopia's Adama Special Khat Shop around Dipo. Then 100 g KWs were washed, dried using sunlight, chopped into smaller pieces, and crushed using a grinder. Cellulose fibers have been extracted from the khat waste, according to Gabriel et al., (2021). 50 g of KW in 500 mL of solution was soaked with 80% w/v of formic acid and 80% w/v of acetic acid at volume ratios of 70/30 in a water bath at 90˚C for 90 minutes. Following repeated washing and filtration steps, the pulp material was then treated with a 2.5% sodium hydroxide (NaOH) solution in a 500 mL volume for one hour. Subsequently, a 500 mL solution mixture comprising 20% formic acid, 20% acetic acid, and 7.5% hydrogen peroxide in a 2:1:2 ratios were added. This mixture was then heated in a water bath maintained at 90°C for 1.5 hours. This was followed by continuous washing of the material with hot water. A bleaching process was then carried out using a 10% hydrogen peroxide solution in an alkaline medium, achieved by adding 20 grams of sodium hydroxide. This was done at a 1:10 fiber to solution ratio at room temperature. After the bleaching treatment, the pulp material was continuously rinsed with hot distilled water. The washed pulp was then dried in oven maintained at 80°C for 24 hours and stored as cellulose fibers for further uses. The percent of yield was calculated according to above equation 1.

$$\text{percent of yield} = \frac{\text{Initial mass} - \text{Final mass}}{\text{Initial mass}} * 100\% \qquad (1)$$

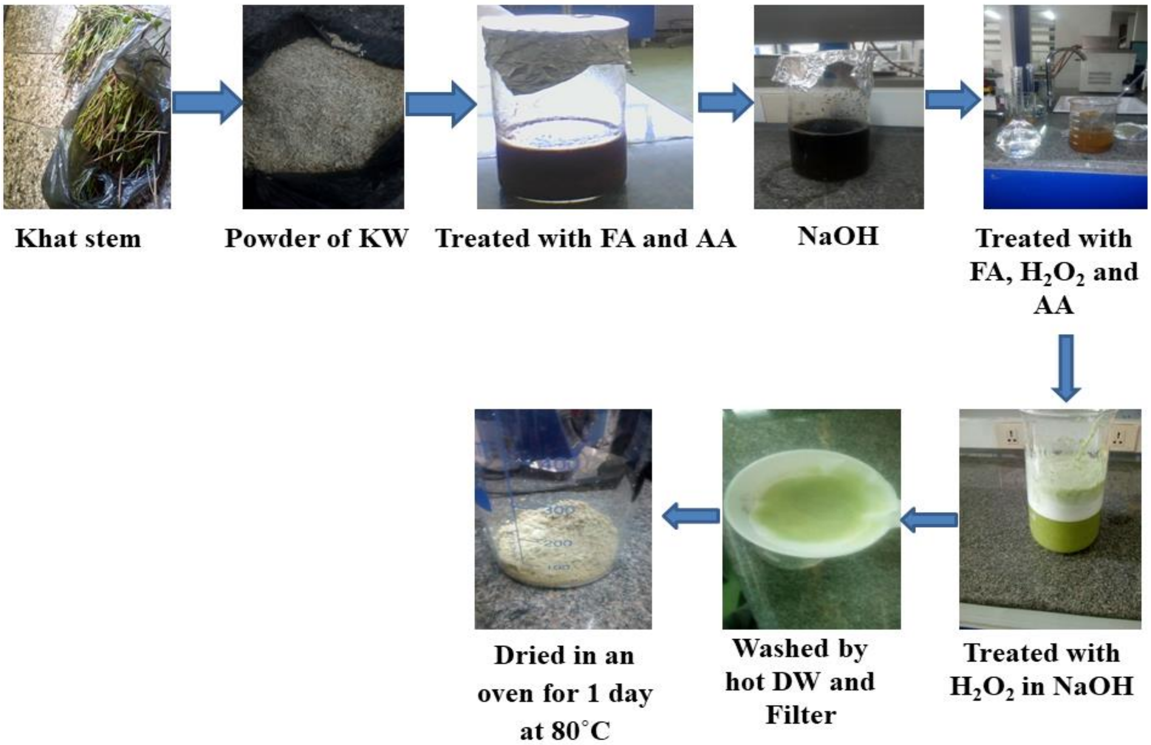

Figure 3: Scheme of cellulose extraction from khat stems methodology.

3.2.2. Synthesis of Nanocellulose

The cellulose-based suspension was then transformed into nanocellulose through an acid hydrolysis process., according to Wulandari et al., (2016) with some modifications. 10 g of cellulose suspension was transferred to a beaker then 100 mL of a 50% aqueous solution of H_2SO_4 was added. The resulting mixture was allowed to soak at room temperature for 90 minutes. The acid hydrolysis reaction was quenched by introduction of ice cold distilled water into the mixture (500 mL) and washed until a pH reached 7. The resulting colloidal suspension was centrifuged, and washed five times using a centrifugation process (1000 rpm, for 10 min). The produced NC was dried at room temperature, weighted and kept in the refrigerator for further analysis. The percent of yield was calculated according to above equation 1.

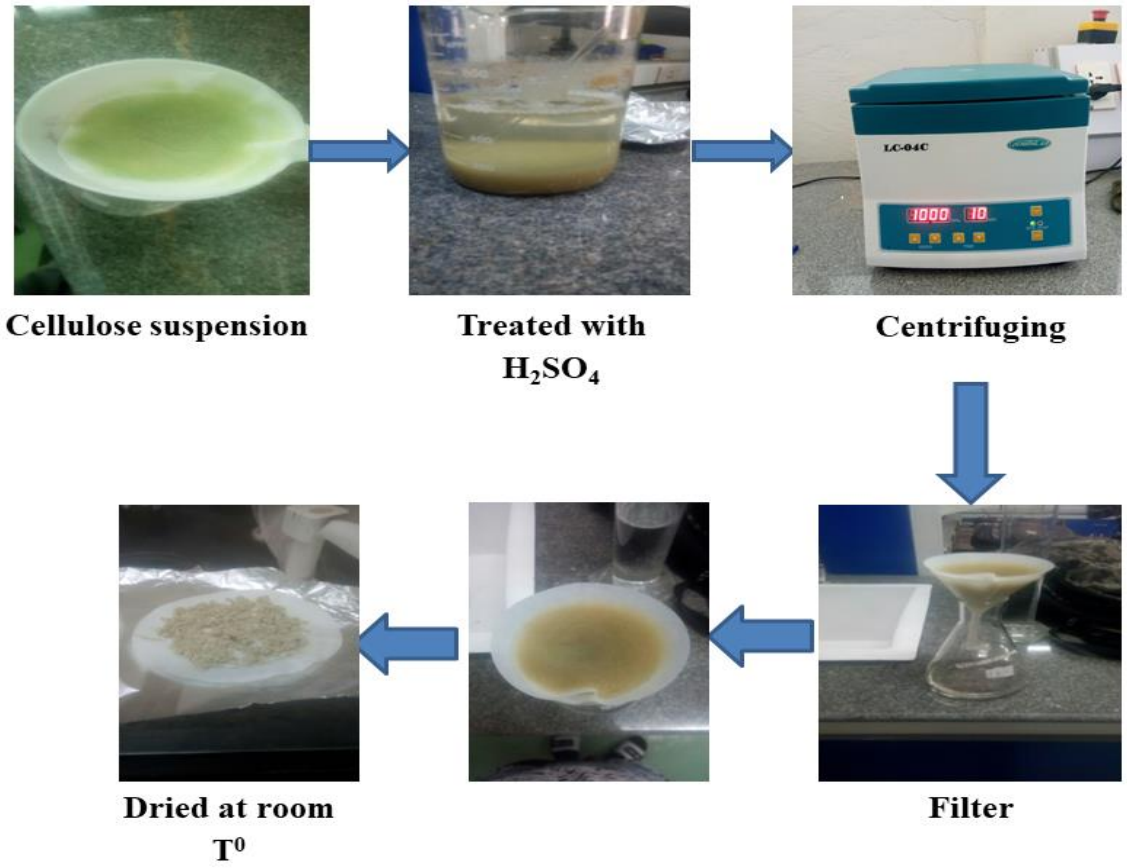

Figure 4: Scheme of nanocellulose preparation method.

3.2.3. Synthesis of Magnetite Impregnated Nanocellulose Composites (MNC)

MNC were synthesized according to Amiralian et al., (2020) with some modifications. 2.3 g sample of the produced NC was added to 200 mL of distilled water, and stirred in magnetic stirrer for 30 minutes at 25^0c. Next, $FeCl_2.4H_2O$ and $FeCl_3.6H_2O$ at 1:2 M were added and stirred at a speed of 700 rpm for one hour. Following, 1 M of sodium hydroxide solution was added until a pH of the solution reached 11. The solution quickly changes the color from light brown to black. This process confirms the formation of nanocellulose magnetite nanocomposite (MNC). The prepared MNC was washed with ethanol and distilled water repeatedly. Finally, the MNC was dried in an oven for one dye at 50^0C, then ready for characterization and adsorption application.

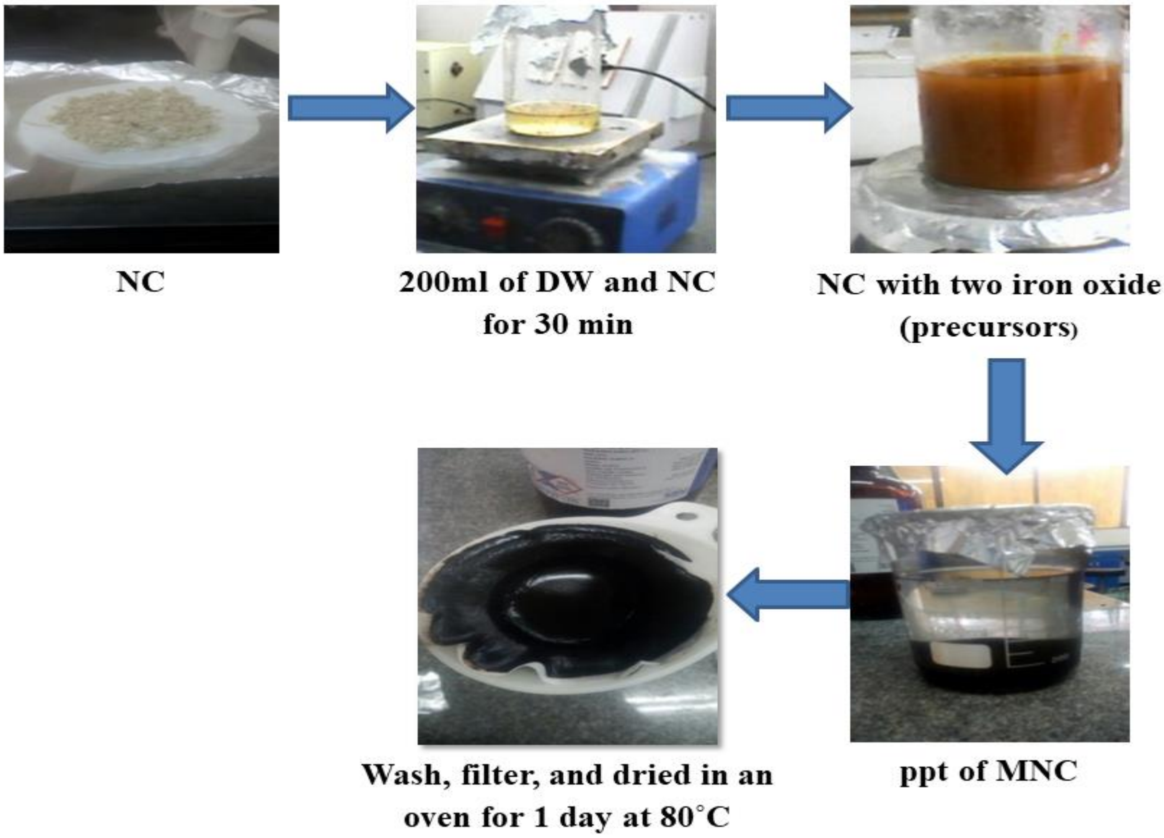

Figure 5: Scheme of magnetite impregnated nanocellulose synthesis methodology.

3.3. Preparation of MB dye Stock Solutions

A stock solution of methylene blue (MB) dye was prepared by dissolving 1 gram of MB in 1000 mL of distilled water, resulting in 1000 mg/L concentrations. The working concentrations (10 – 200mg/L) were then prepared from this stock solution using Equation 1.

$$C_1 V_1 = C_2 V_2 \qquad (2)$$

The concentration of the methylene blue (MB) dye was measured using a UV-visible spectrometer at 664 nm. A calibration curve was then plotted, relating the absorbance to the concentration of the dye solution, in order to obtain the absorbance-concentration relationship.

3.4. Characterization of prepared materials

3.4.1. Differential Scanning Calorimetriy (DSC) Analysis

Differential scanning calorimetry (DSC) is a thermal analysis technique that measures the temperature and heat flow associated with material transitions as a function of temperature and time. These measurements provide quantitative and qualitative data on the physical and chemical changes occurring in the sample, such as endothermic/exothermic processes or variations in heat capacity. Specific data that can be acquired include glass transition temperature, melting temperature, and the thermal stability of samples (Fatahi et al., 2022). The DSC machine was calibrated using voltage in uW versus temperature. Approximately 8 mg of sample (NC and MNC) was used for analysis and heated from 33-550°C at rate of 10°C/min under N_2 environment against vacuumed reference pan. This analysis was conducted at Addis Ababa Science and Technology University, central laboratory.

3.4.2. X-ray Diffraction (XRD) Analysis

XRD used to analyze structure of the synthesized cellulose, Fe_3O_4, NC, and MNC. The XRD analysis was to determine if the produced materials were crystalline or amorphous. The Debye Scherer formula was used to get the average crystalline size (Muswareen et al., 2023).

$$D = \frac{0.94\lambda}{\beta \mathrm{Cos}\theta} \tag{3}$$

Where: Where the X-ray source wavelength $\lambda = 1.54$ A^0, crystallite size (D), full width at half maximum (FWHM) of a peak (β), and peak position (θ). The Department of Material Engineering at Adama Science and Technology University performed XRD investigation on produced materials. The Shimadzu XRD-7000 X-ray diffractometer was used to draw the X-ray diffraction patterns of the dried powder of the synthesized samples. The X-ray source used was copper emission, with a nickel filter and a wavelength of 1.5418 Å. The samples were scanned within a 2θ range between 10 and 80 degrees.

3.4.3. Fourier Transform Infrared spectroscopy (FTIR) Analysis

In order to identify functional groups of khat stem, cellulose, NC, and MNC FTIR spectroscopy was utilized. The Chemical Department at Addis Ababa Science and Technology University conducted an FTIR analysis on the produced materials. The dried powder of the produced materials was examined to get FTIR spectra in the 4000-400 cm^{-1} range.

3.4.4. Scanning Electron Microscopy (SEM) Analysis

The scanning electron microscope (SEM) is a versatile instrument that belongs to the electron microscope category that is often used to examine very large-dimensional subsurface samples or surfaces with polished or rough surfaces (Wallyn et al., 2019). The Adama Science and Technology University biology department was performed the SEM analysis on the NC and MNC, providing direct imaging of exterior morphological information. A small amount of powder was used. Due to their less conductive nature, NC and MNC need coating with a conductive substance using a sputter coater, taking a gold alloy as a coater.

3.4.5. BET Surface Area, Pore Volume, and Pore Size Analysis

Multipoint BET approach was used to determine NC, magnetite, and MNC surface areas. N_2 adsorption measurements are used in the Brunauer-Emmett-Teller (BET) method to estimate the surface area of synthetic materials (Mohan et al., 2020). The analysis was conducted in the Department of Chemistry at Bahirdar University.

3.4.6. Determination of Concentration of MB by UV-Vis Spectrophotometer

UV-Vis spectrophotometer was used to determine the concentration of methylene blue dye in solution. Solutions with gradually increasing concentrations from 2 to 10 mg/L were prepared, and their absorbance wavelength (664 nm) was measured to build the calibration curve. A linear graph of absorbance against concentration was developed, and the straight-line's equation was identified. The data obtained from UV-visible spectrophotometry experiments were used for optimization parameters (adsorbent dose, contact time, solution pH, and initial concentration) at maximum wavelength of the MB in the batch adsorption studies.

3.5. Batch Adsorption Studies

The adsorption experiment for methylene blue (MB) dye on MNC was performed using a magnetic stirrer. The experiment utilized 100 mL of an aqueous MB dye solution with an initial concentration of 10 mg/L. 0.1M HCl or 0.1M NaOH was used to adjust the pH of solutions. In all studies, the flasks were covered by aluminum foil to prevent any reactions during the experiment. After allowing the solutions to reach equilibrium by shaking the flasks, the adsorbents were separated from the supernatant solution through filtration. The concentration of the filtered MB solution was then analyzed using a UV-visible spectrophotometer, which measured the changes in absorbance at the wavelength of maximum absorbance. To investigate the effects of various parameters on the adsorption of MB dye on MNC, all other parameters were maintained at constant and optimized values during the individual parameter studies. For all the parameters, a percent of adsorption (%) was calculated using the following equation:

$$\text{Percent of adsorption (\%)} = \frac{C_o - C_e}{C_o} * 100 \qquad (4)$$

Adsorption capacity was calculated by equation 4:

$$Q = \frac{(Co - Ce)V}{M} \qquad (5)$$

Where:

- ✓ C_0: Concentration of methylene blue dye in the sample solution before adsorption
- ✓ Ce: Concentration of MB, dye in the sample solution at equilibrium
- ✓ Q- dye adsorption capacity (mg/g)
- ✓ V- volume of the solution (L)
- ✓ M- amount of adsorbent (g).

3.5.1. Effect of contact time

Contact time effect on the cationic MB dye removal efficiency was determined by varying the contact time in the range of 15-120 minutes and in 100 mL of MB solution while keeping other parameters initial concentration (10 mg/L), solution pH=8 and adsorbent dosage of 0.03 g at constant value. Solution was stirred for different contact times at 300 rpm, once the reaction had finished, the resulting mixture was meticulously. Ultimately, measurement of MB solution was carried out using a UV-VIS spectrometer.

3.5.2. Effect of adsorbent dose

Effect of adsorbent dosage on cationic MB dye removal was determined by changing the amount of MNC in range of 0.01-0.1 g in a 100mL of solution through keeping other parameters (initial concentration at 10 mg/L, and solution pH=8) at constant and contact time at optimized value. The solution was stirred for 80 minutes at 300 rpm, then after the reaction was completed, it was carefully filtered. Ultimately, the measurement of MB solution was carried out using a UV-VIS spectrometer.

3.5.3. Effect of solution pH

To investigate how pH affects MB dye adsorption, 0.07 g/100mL of MNC was added to 10 mg/L of MB dye initial concentration at a constant value. Then, a pH of solutions was varied between 2, 4, 6, 7, 8, 9, and 10 while maintaining optimized values for contact time, and adsorbent dose. Following an 80 minutes stirring period at 300 rpm, then the solution was thoroughly filtered. Ultimately, the measurement of MB solution was carried out using a UV-VIS spectrometer.

3.5.4. Effect of concentration

Effect of initial adsorbate concentration on MB removal was determined by varying the amount of initial MB dye concentration in range of 10-50 mg/L by keeping other parameters at optimized value. The solution was stirred for 80 minutes at 300 rpm, and once the reaction had finished, the resulting mixture was meticulously filtered using filter paper. Ultimately, the measurement of this solution was carried out using a UV-VIS spectrometer.

3.6. Adsorption Isotherm

The adsorption isotherm depicts the correlation between the quantity of material accumulated at a fixed temperature and its concentration in the balanced solution. The experimental results on adsorption are described using equilibrium isotherm equations. The data obtained from the equilibrium isotherm equation offers insights into the adsorbent's capacity, or the amount needed to remove a unit mass of pollutant under the given system concentrations (M. T. Uddin et al., 2017). Langmuir isotherm and Freundlich isotherm are the surface adsorption models most frequently utilized for single-solute systems (Al-Degs et al., 2007). In this work, the two most common isotherm equations have been used to assess solute equilibrium data between adsorbent and adsorbate. The insights gained from these different adsorption models offer valuable information about the adsorption mechanisms, the surface properties of the adsorbent, and the adsorbent's affinities. Linear regression is commonly used to determine the isotherm that provides the best fit, and applicability of the isotherm equations was evaluated by calculating the correlation coefficients (Tan et al., 2008). Adsorption isotherms were conducted at an initial methylene blue (MB) concentration range of 10-200 mg/L, a pH of 8, a sorbent amount of 0.07g/100mL, for duration of 80 minutes at room temperature.

3.6.1. Langmuir Isotherm Model

Langmuir isotherm applies to adsorption of a solute from a liquid solution can be described as a monolayer adsorption process, where the solute is adsorbed onto a surface with fixed number of identical adsorption sites. The Langmuir isotherm model presumes the adsorption energy is uniform across the surface, and there is no migration of the adsorbate within the plane of the surface (Saadi et al., 2015). The experimental findings were assessed through the linear formulation of the Langmuir isotherm model. Linear plots of Ce/qe VS Ce suggest that the Langmuir isotherm model is applicable for the removal of methylene blue dye. The Slopes and intercepts of the linear plot (Ce/qe VS Ce) were used to calculate values of qe and KL of the Langmuir adsorption isotherm (Khaled et al., 2009). Equation 5 gives the Langmuir model (Nebaghe et al., 2016).

$$\frac{\mathrm{Ce}}{\mathrm{qe}} = \frac{\mathrm{Ce}}{\mathrm{qm}} + \frac{1}{\mathrm{qmKL}} \qquad (6)$$

3.6.2. Freundlich Isotherm Model

The Langmuir isotherm model presumes the enthalpy of adsorption does not depend on the quantity of material adsorbed. In contrast, the empirical Freundlich equation can be derived for adsorption on heterogeneous surfaces by assuming that the enthalpy of adsorption decline logarithmically as fraction of occupied sites increase. The Freundlich equation is an empirical model, based on adsorption on heterogeneous surfaces, it often expressed as a nonlinear equation. Linear plot of log qe VS log Ce yielded Kf and 1/n as intercepts and slopes. The Freundlich model is represented by equation 6:

$$\text{Log qe} = \text{logKf} + \frac{1}{n}\text{log Ce} \tag{7}$$

In equations 6 and 7, Ce-equilibrium concentration of MB (mg/L), qe-equilibrium adsorption capacity (mg/g), KF-Freundlich constant related to adsorption capacity, KL-Langmuir constant related to the free energy of adsorption (mg/L), qm-maximum adsorption capacity (mg/g), and n-adsorption intensity.

3.7. Adsorption kinetics model

Kinetic models were employed to investigate the controlling mechanisms of the sorption process, which include diffusion control, chemical reactions, and mass transfer. Also used to express the adsorption mechanism chemisorption or physisorption depends on the calculated data's. Understanding the process rate and the factors that influence it is crucial. To achieve this, the kinetics of the process were analyzed (Wakkel et al., 2019). The adsorption kinetics of methylene blue (MB) on MNC were evaluated using the pseudo second order and pseudo first order kinetic model approaches. In this study, a kinetic analysis of methylene blue removal was conducted to understand the behavior of the prepared low-cost adsorbent.

3.7.1. Pseudo First Order and Pseudo Second Order Kinetic Models

The pseudo first order kinetic model presumes the rate of adsorption site occupation is directly proportional to the quantity of unoccupied adsorption sites. The plot of ln (qe-qt) against t was found to be linear. The slopes and intercepts of ln (qe-qt) against the t plots were used to calculate values of K1 and qe with pseudo first order kinetic equations and various parameters. The pseudo first order kinetic model, which is widely utilized to forecast the adsorption rate based on the adsorption capacity, was employed in this study. (Revellame et al., 2020), can be expressed by equation 8:

$$\ln(\text{qe} - \text{qt}) = \ln\text{qe} - \text{K1t} \tag{8}$$

Where: Where qt (mg/L)-amount of adsorbrate at time t (min), qe (mg/L)-amount of the adsorbate at time under equilibrium conditions, and k1-pseudo first order rate constant

(min^{-1}). When studying adsorption kinetics, the pseudo first order and pseudo second order models are frequently employed to fit the experimental data. The linear form of the pseudo first order model is expressed by equation 9 (Moussout et al., 2018):

$$\frac{t}{qt} = \frac{1}{K2qe2} + \frac{1}{qe} \tag{9}$$

Where, qe and qt are the adsorption capacities corresponding to the equilibrium and time t , respectively with expressed units of mg/g, t is contact time (minutes), K2 is pseudo second order constant (mg/gh), and K1 is pseudo first order constant (h^{-1}). These kinetic experiments were carried out at optimized contact time, with an initial methylene blue (MB) concentration of 10 mg/L, a pH of 8, an adsorbent dose of 0.03 g/100mL, and a continuous speed of agitation at 300 rpm. The remaining methylene blue dye concentration in solution was measured by taking samples at 15 minute intervals during the timeframe of 15 to 120 minutes. The data from the experiment was then utilized to compute the pseudo first order and pseudo second order kinetic models.

3.8. Reusability of MNC

To investigate reusability of MNC, added a mass of 0.07 g of MNC to 100 mL of a 10 mg/L initial MB concentration at a pH of 8. The solutions were agitated for 80 minutes at 300 rpm, and after reaction was completed, the MNC was carefully collected using an external magnate. The recovered MNC was washed 3 times with ethanol and once by water. Afterward, the MNC was dried for duration of 24 hours. The above procedures were repeated five times. Finally, the measurement of the MB in the solution was carried out using UV-Vis spectroscopy.

CHAPTER FOUR

4. RESULT AND DISCUSSIONS

4.1. Physical Properties of KW, Cs, NC and MNC

The color of cellulose fibers and nanocellulose in Figure 6 (b and c) was likely white as compared to KW (Figure 6a), which represents removal of non-cellulosic components from prepared materials. The removal of non-cellulosic components led to an increase in yield of cellulose in the extracted cellulose fiber. The percent of yield of cellulose and nanocellulose was calculated according to equation 1 and the cellulose content of the KW increment ranges from 30% to 85%. The yield of cellulose fiber from KW in this study was decreased as compare to the yield of Gabriel et al., (2021) from 39.4% to 30% may be due to random and systematic or conditions where experiments was done. The purpose of using formic acid and acetic acid in the pretreatment step was to enhance the purity of the extracted cellulose. Furthermore, it facilitates the removal of lignin enhances the whiteness of the pulps. Figure 6 (d) shows color of MNC was black because impregnation of Fe_30_4 in the nanocellulose suspension made it change color from white to black.

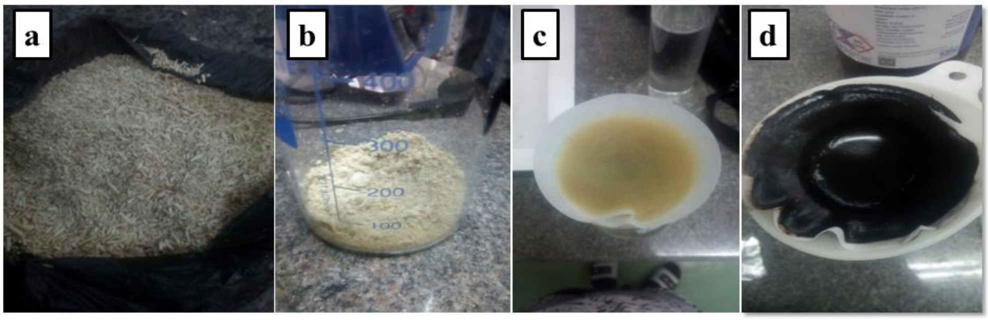

Figure 6: Scheme of prepared materials khat waste (a), cellulose (b), nanocellulose (c), and magnetite impregnated nanocellulose (d).

4.2. Characterization of Prepared Materials

4.2.1. DSC Analysis

The DSC (Differential Scanning Calorimetry) results for NC (material) and MNC (material) are shown in figure 7. Glass transition temperature (Tg) of NC and MNC was observed at around 34.9^0c and 51.1^0c, respectively. This indicates that as the materials are heated, the amorphous regions transition from a brittle glassy state to a more flexible rubbery state (Kalogeras & Hagg Lobland, 2012). The Tg of MNC was higher than NC, which indicating that the amorphous regions of MNC have higher thermal stability and require more energy to transition from a glass state to a rubbery state. The DSC analysis revealed two endothermic peaks for both NC and MNC. The first, lower endothermic peak observed below 300.8°C for NC and 274.7°C for MNC was attributed to the evaporation of bound water from the respective samples. The samples exhibited more pronounced second transition peaks at around 403.6°C and 378.5°C, which corresponded to the melting of the nanocellulose (NC) and MNC components present in the material, respectively. The same result was reported by S. Rashid & Dutta, (2020). Also, one exothermic peak was observed around 370°C and 341.3°C for NC and MNC, respectively. This indicates the release of heat from the sample. The thermal stability of NC and MNC started around 457.8°C and 410°C, respectively. After this point, there weren't any endothermic or exothermic peaks, which indicate that thermal stability of synthesized materials started at this point. From this data thermal stability of MNC was higher than NC According to all of the above data; MNC was more thermally stable than NC, which indicates that the impregnations of magnetite nanoparticles into nanocellulose enhance the thermal stability of MNC.

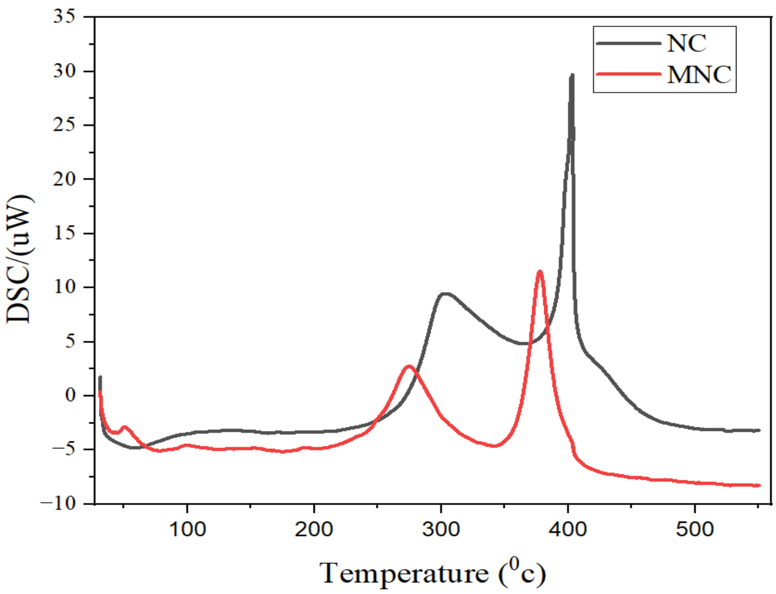

Figure 7: DSC/ (uW) plot of nanocellulose (NC), and magnetite impregnated nanocellulose (MNC).

4.2.2. XRD Analysis

The XRD spectra displayed peaks (as shown in Figure 8a) at 2θ values of 16.6°, 22.6°, and 34.5°, which are characteristic of the typical cellulose I structure and can be assigned to the (110), (200), and (004) crystallographic planes, respectively. The same result was reported by Nam et al., (2016). The spectral analysis revealed the amorphous and semi-crystalline nature of the cellulose, indicating a reduced degree of crystallinity (Kara, et al., 2021). The XRD analysis determined the crystalline structure of the synthesized magnetite nanoparticles based on the characteristic peaks observed. It was found that all the reflection peaks (Figure 8b) at 2θ of 18.4°, 30.4°, 35.5°, 43.2°, 53.9°, 57.2°, 62.8°, and 74.2° assigned to (111), (220), (311), (400), (422), (511), (440), and (533) planes can be indexed by the cubic inverse spinel structure of the magnetite iron oxide nanoparticles. The same result was reported by Nurbas et al., (2017) and W. Kim et al., (2012). The diffraction patterns of Fe_3O_4 NPs were found to be in good agreement with JCPDS card number 00-019-0629, which confirms the formation of pure Fe_3O_4 NPs without the formation of any secondary phase. The XRD analysis of the nanocellulose-magnetite composites revealed a captivating diffraction pattern (Figure 8b). Distinct peaks were observed at 2θ angles of 16° and 22.6°, which correspond to the (110) and (200) planes - a telltale signature of the typical cellulose I structure. The spectrum also showcased a series of reflection peaks at 2θ values of 30.4°, 35.5°, 43.2°, 53.9°, 57.2°, 62.8°, and 74.2°. These can be attributed to the (220), (311), (400), (422), (511), (440), and (533) planes, collectively painting a vivid picture of the crystalline structure of the magnetite nanoparticles embedded within the nanocellulose matrix. This intriguing XRD fingerprint illuminates the successful integration of these two captivating materials. The average crystalline size of the MNC and magnetite was calculated in Table 2 according to equation (3). The average crystalline sizes of MNC and magnetite were 8.02 nm and 11.75 nm, respectively. From the calculated data, MNC has a smaller crystalline size as compared to magnetite; this is due to the amorphous nature of nanocellulose, as observed in Figure 8 (a). However, the amorphous nature of NC in MNC (Figure 8b) decreased due to impregnation of Fe_30_4. According to El-Nahas et al., (2017), when NC was combined with magnetite, the crystalline nature of NC increased.

Table 2: Average Crystallite Size (D) of MNC and magnetite

MNC				Magnetite			
No Peaks	**2θ**	**FWHM**	**D**	**No Peaks**	**2θ**	**FWHM**	**D**
1	35.7647	0.895	9.75 nm	1	35.6122	0.7187	12.13 nm
2	22.5494	1.9867	4.26 nm	2	62.8259	0.835	11.65 nm
3	63.008	0.97	10.04 nm	3	30.248	30.248	11.46 nm
Average Crystallite Size = 8.017 nm				**Average Crystallite Size** = 11.747 nm			

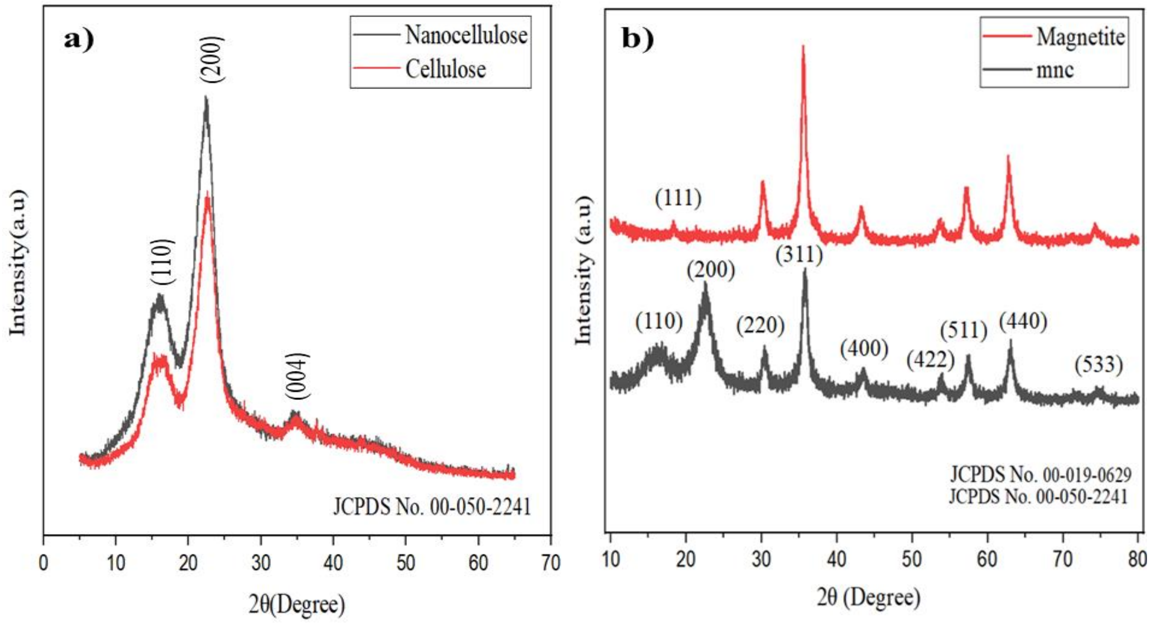

Figure 8: XRD Spectrum of nanocellulose and cellulose (a), and magnetite and MNC (b).

4.2.3. FTIR Analysis

The information on the functional groups of KW, cellulose, NC, and before and after adsorption of MNC adsorbents was determined by FTIR spectroscopy (Lingegowda et al., 2013). Figure 9 (a, and b) shows FTIR spectrum of khat stem, cellulose, nanocellulose, and MNC (before and after adsorption). From those indicated peaks, the broad absorption peak observed approximately at 3330 cm^{-1} (Figure 9a) indicates the presence of O-H stretches. In Figure 9(a), due to the asymmetric stretching vibration of the CH_2 bond, there is a weak band around 2899 cm^{-1}. The peak observed around 896 cm^{-1} is attributed to the CH rocking vibration of cellulose, which is indicative of the presence of β-glycosidic linkages. Bands observed around 3330 cm^{-1}, 2899 $^{-1}$, and 896 cm^{-1} in the cellulose and nanocellulose (NC) spectra are characteristic of cellulose I, indicating that the chemical structure of the cellulosic fragments was not affected by the acid hydrolysis process. The same result was reported by Gabriel et al., (2021). The disappearance of the peak (Figure 9a) around 1735 cm^{-1} for cellulose and NC indicates during chemical treatment of the material the cleavage of linkages between ferulic acid or p-coumaric acid and the lignin (Reddy et al., 2013). In Figure 9(a), the disappearance of the bands around 1228 cm^{-1} from cellulose fibers and NC indicates the dissociation and dissolution of lignin functional groups such as aromatic rings (Gabriel et al., 2021). Due to the using of formic acid and acetic acid in extraction process, the above two data shows that the disappearances of lignin and hemicellulose during extraction of cellulose fibers. In Figure 9(b) the board absorption bands around 3350 cm^{-1} indicate OH stretching, and weak band around 1633 cm^{-1} represent β-glycoside bonds (C=O). The peak (Figure 9b) around 547 corresponds to vibration of Fe-O bond, which indicates the Fe_30_4 phase. The same result was reported by Jodeh et al., (2018). After the adsorption of methylene blue dye (MNC + MB), the board band around 3329 cm^{-1}, weak band around 2902 cm^{-1} and bending around 1029 cm^{-1} may indicate adsorption of methylene blue dye onto the MNC.

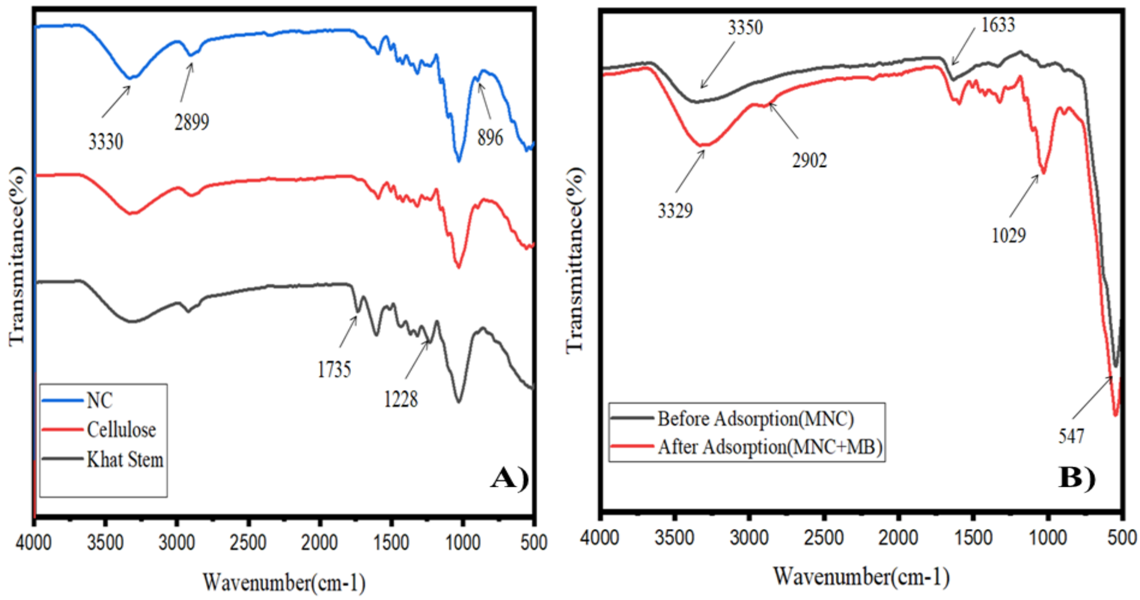

Figure 9: FTIR spectrum of NC, cellulose and khat stem (A), and before adsorption (MNC) and after adsorption (MNC + MB).

4.2.4. SEM Analysis

Figure 10 (A and B) shows SEM micrographs of the synthesized nanocellulose adsorbent. The SEM images demonstrated that the nanocellulose adsorbent had a fibrous structure and shape, with slightly rough surface texture and a heterogeneous pore spread throughout its matrix. The observed roughness of the nanocellulose adsorbent's surface is attributed to the removal of impurities such as waxes and oils, as well as the removal of most of the non-cellulosic components like lignin and hemicellulose, through the chemical treatment process (Zamboni et al., 2023). According to the findings reported by Mokaloba & Batane, (2014), the increased roughness of the fibers after mercerization leads to an enhancement in the specific surface area of the fibers, which in turn results in greater adherence. The nanoscale roughness of the cellulose surface in Figure 10 (C) was derived from Fe_3O_4 NPs (Y. Zhang et al., 2019). The micrograph of the MNC composite in Figure 10(C) shows a distribution of white and black surfaces on the composite surface. This suggests that the nanocellulose (CN) and the iron oxide nanoparticles were dispersed within the composite, while some agglomeration of the magnetite nanoparticles was also observed. Same result was reported by Evans et al., (2022).

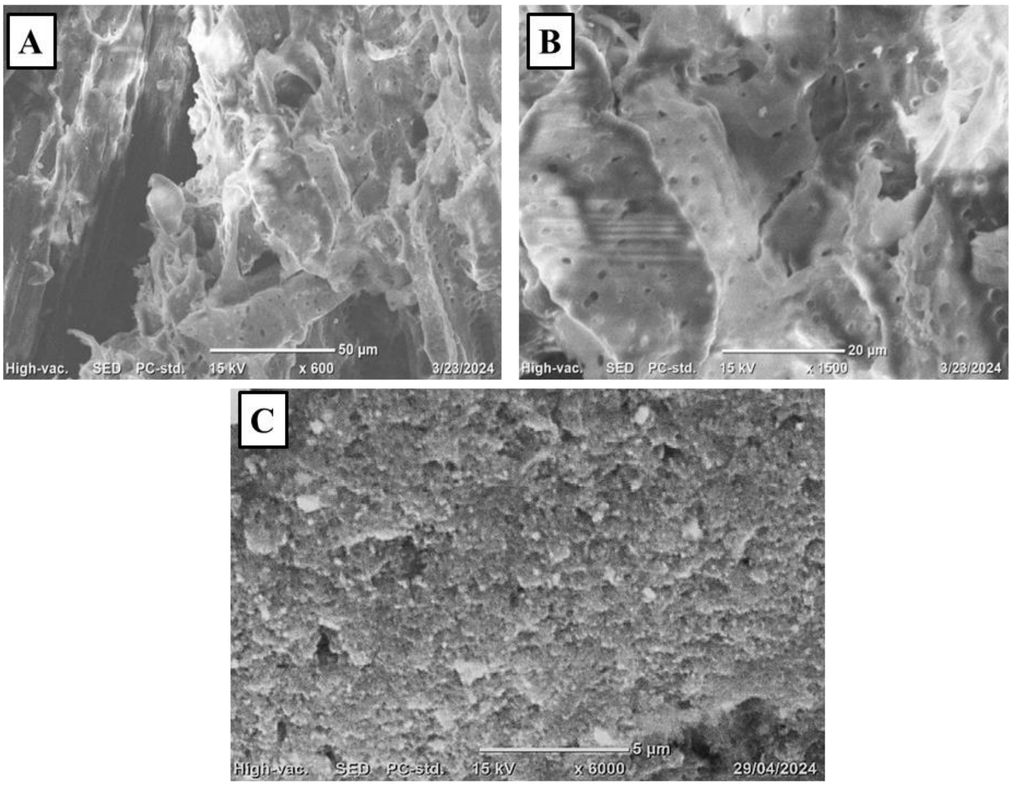

Figure 10: SEM analysis of nanocellulose at 50 µm (A), nanocellulose at 20 µm (B), and magnetite impregnated nanocellulose (C).

4.2.5. BET Surface Area, Pore Volume, and Pore Size Analysis

The BET method was used to analysis the surface area, total pore volume, also average pore size of the NC, MNC, and magnetite. Figure 11 shows direct linkage between quantity adsorbed and relative pressure; as relative pressure increased, quantity adsorbed also increased. Table 3 presents average pore size, total pore volume, and BET surface area measurements for the prepared adsorbent materials. The average pore size of NC, magnetite, and MNC was 1.304 nm, 0.578 nm, and 0.619 nm. The average pore size of MNC was higher than that of magnetite and smaller than that of NC. Pore sizes of all prepared materials were presented in Table 3; which revealed the microporous nature of the nanocomposites. The multi-point surface area of NC, magnetite, and MNC was 536.27 m^2/g, 613.67 m^2/g and 511.74 m^2/g, respectively. Surface area of NC was increased, but when impregnated by magnetite, it decreased. This may be caused by the agglomerations of magnetite in MNC, as seen in the SEM image (Figure 10 C). The NLDFT cumulative surface area of NC, magnetite, and MNC was 123.2 m^2/g, 234.5 m^2/g and 154.1 m^2/g, respectively. In the current situation, the surface area of MNC was higher than that of NC. Generally, MNC has a higher surface area and average pore size, which indicates the MNC, is best for the adsorption of MB dyes.

Table 3: BET surface area, total pore volume, and average size.

Prepared Materials	Surface Area Multi Point BET (m^2/g)	NLDFT cumulative surface area(m^2/g)	Total Pore Volume (*10^{-1} cc/g)	Average Pore Size (nm)
Nanocellulose	536.270	123.2	0.919	1.304
Magnetite	613.670	234.5	1.936	0.578
MNC	511.735	154.1	1.335	0.619

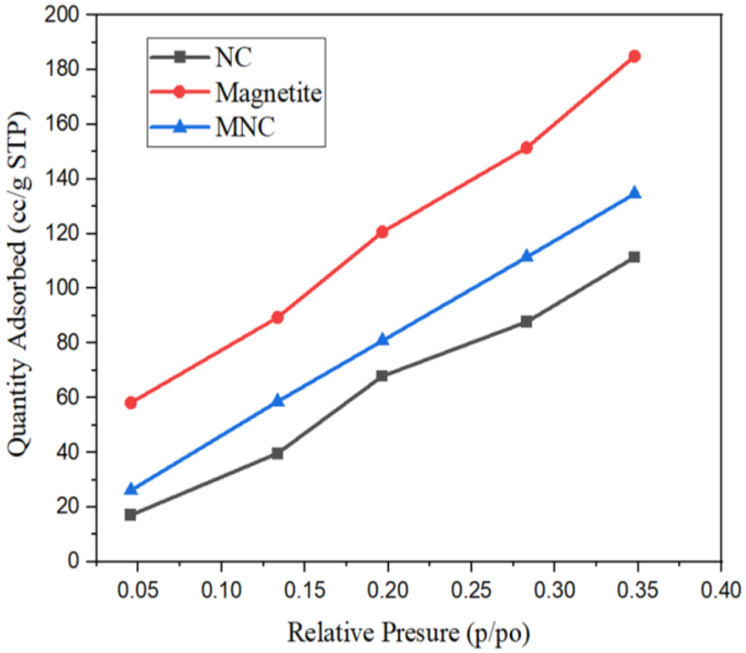

Figure 11: BET quantity adsorbed (cc/g) VS relative pressure (p/po) plot of nanocellulose, magnetite, and MNC.

4.2.6. Determination of Concentration of MB by UV-Vis Spectrophotometer

The calibration curve was generated to figure out the concentration of methylene blue (MB) dye in an aqueous solution using UV-Vis spectrophotometer. The calibration curve was created by producing solutions with gradually increasing concentrations and measuring their absorbance. MB absorbs ultraviolet Visible light at wavelength of 664 nm. A linear graph of absorbance versus concentration was plotted, and the equation of the resulting straight line was determined. Samples from the adsorption studies were analyzed, and their absorbance values were measured. The concentrations of the solutions were then determined by referring to the calibration graph. Here, Figure 12 shows the linear calibration curve plot of MB dye.

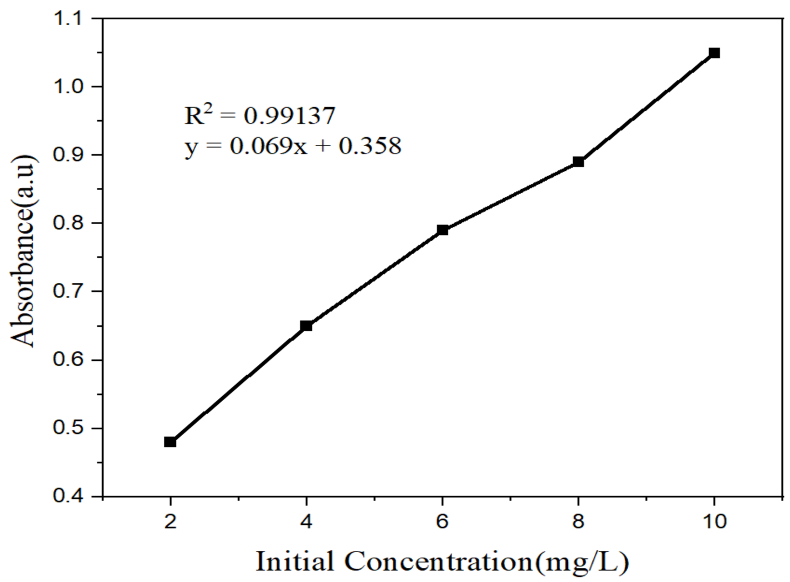

Figure 12: Calibration plot of methylene blue dye absorbance versus initial concentration.

4.3. Batch Adsorption Studies

4.3.1. Effect of Contact Time

Figure 13 (a and b) shows the percent removal and adsorption capacity of MNC. The percentage of removal and adsorption capacity rise as the contact time increased, and as the contact time increased, the reaction rate also increased. The adsorption process reaches a point where the amount of MB desorbing from the adsorbent equals the amount being adsorbed, resulting in a constant value beyond which no further removal occurs from the solution. This state of dynamic equilibrium is attained after a specific duration, known as the equilibrium time, and the quantity of MB adsorbed at this equilibrium point represents the maximum adsorption capacity of the adsorbent under the given operating conditions. In this study, the equilibrium was observed to be established after 80 minutes. This can be attributed to the initially high rate of MB uptake, as all the adsorption sites were vacant and the MB concentration was elevated. However, as the adsorption sites became occupied over time, the uptake rate declined (H. Wang et al., 2016). Figure 16 (c and d) shows the absorbance spectra decreased as the contact time increased and the color fade of MB as the contact time increased, respectively. The percent removal efficiency and adsorption capacity were calculated according to equations (4) and (5), respectively. Table 4 shows the percent removal and adsorption capacity at different contact times.

Table 4: Effect of initial concentration on percent removal and adsorption capacity of methylene blue dye

Contact Time (Min)	**Removal Efficiency (% removal)**	**Adsorption Capacity (mg/g)**
15	67.7	22.57
30	73.45	24.48
45	78.57	26.19
60	82.1	27.37
80	87.85	29.28
100	87.9	29.3
120	87.98	29.33

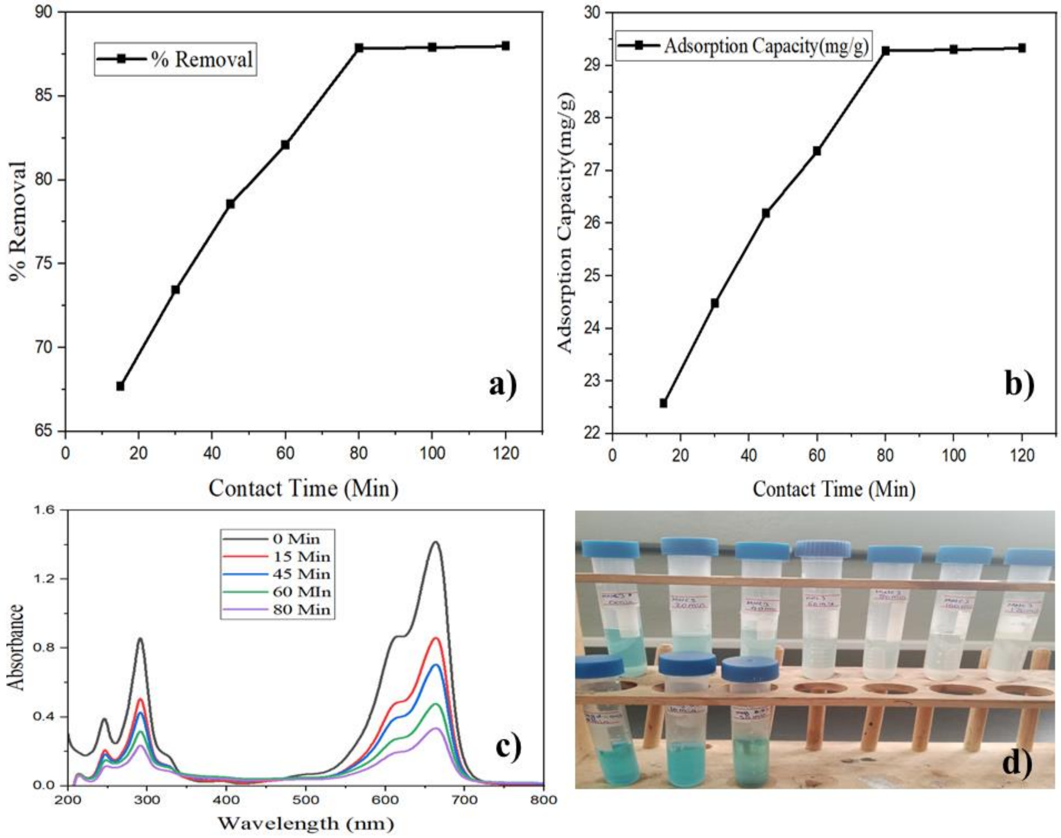

Figure 13: Effect of contact time on methylene blue dye adsorption (a) removal efficiency (%),(b) adsorption capacity (mg/g), (c) absorbance spectrum at different contact time, and (d) color fade of MB dye (pH = 8, amount of sorbent 0.03g/100mL, 25 ^{0}c).

4.3.2. Effect of Adsorbent Dose

Effect of adsorbent dosage was investigated by holding all other parameters constant, including pH = 8, initial methylene blue (MB) dye concentration = 10 mg/L, temperature = 25°C, mixing speed = 300 rpm, solution of 100 mL, and contact time = 80 minutes at the optimized value. Effect of the adsorbent dose was examined by varying amount of MNC from 0.01-0.1 g. The effect of the adsorbent dose on the removal efficiency and adsorption capacity of dye is shown in Figure 14 (a and b). In Figure 14(a), with the increase in adsorbent dose from 0.01 to 0.07 g, the sorption degree of the dye increased. The increase in adsorbent dosage led to a higher number of available active sites for the adsorption of the dye molecules, which resulted in the observed improvement in dye removal (Akperov & Akperov, 2019). The adsorption equilibrium for the dye was achieved at an adsorbent dosage of 0.07 g, and the dye removal remained largely constant above this dosage. Therefore, 0.07 g appears to be the optimum adsorbent dosage for the process. The adsorption capacity (Figure 14b) decreased as the adsorbent dose increased. The reason for this is that as the adsorption process progressed, the active sites on the adsorbent became saturated. This resulted in a decrease in the amount of dye adsorbed per unit mass of adsorbent. This effect was likely associated with a reduction in the available surface area of MNC adsorbent due to aggregation at the higher dosage. As a result, it can be concluded that at a higher mass of MNC, the adsorption process may be ineffective, resulting in increased operational costs. The same result was reported by Handayani et al., (2024). Figure 14(c) shows the absorbance spectra decreased as the adsorbent does increased. The percent removal efficeincy and adsorption capacity were calculated according to equitions (4) and (5), respectively. Table 5 shows percent removal and adsorption capacity at different adsorbent doses.

Table 5: Adsorbent dose effect on removal efficiency and adsorption capacity of methylene blue dye

Adsorbent Dose (g)	Adsorption Capacity (mg/g)	Removal Efficiency (% removal)
10mg/100mL	82.1	82.1
30mg/100mL	29.95	87.85
50mg/100mL	18.2	90.1
60mg/100mL	15.6	93.6
70mg/100mL	13.85	97.03
80mg/100mL	12.15	97.25
90mg/100mL	10.82	97.36

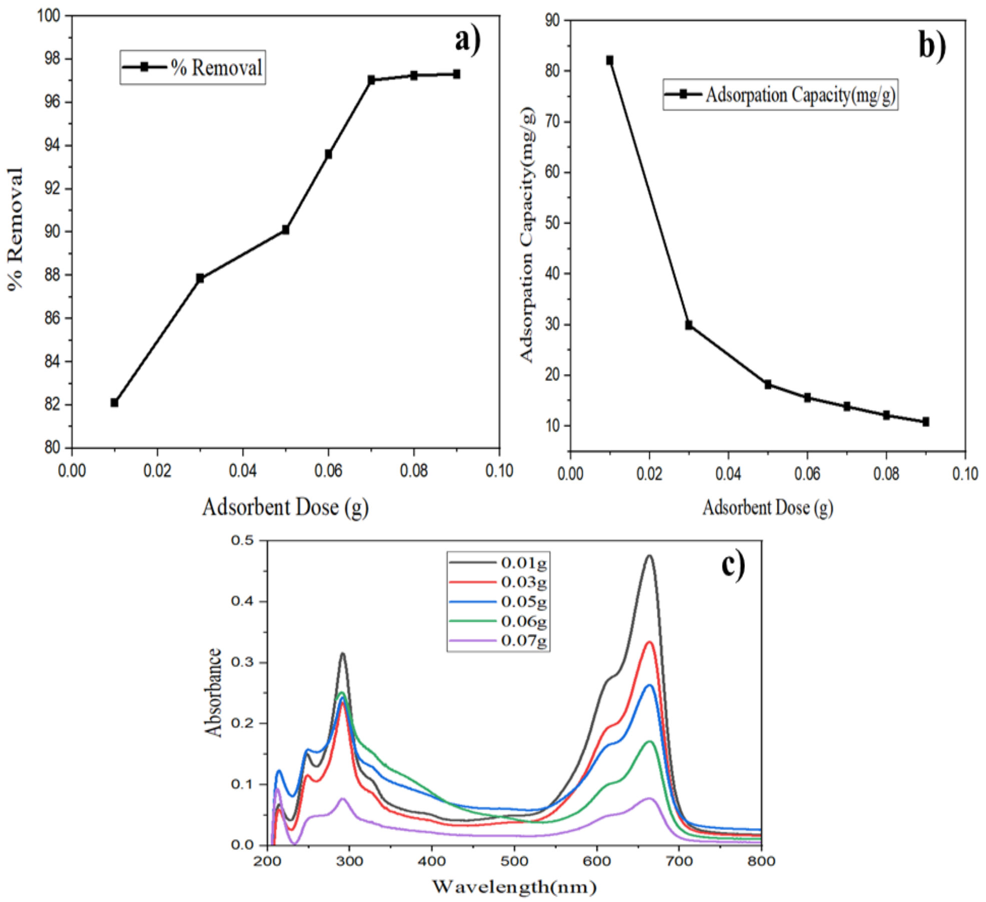

Figure 14: Effect of adsorbent dose on methylene blue dye adsorption (a) removal efficiency (%), (b) adsorption capacity (mg/g), and (c) absorbance spectrum at different adsorbent dose (pH = 8, contact time = 80min, concentration of 100mL at 25^{0}c).

4.3.3. Effect of Solution pH

To determine optimal pH for MB dyes solution, the pH was varied across a range of values, including 2, 4, 6, 7, 8, 9, and 10. Figure 15 (a and b) shows the percent removal and adsorption capacity of MNC at different pH values. The maximum pH was reached at a pH of 8, and the lowest was at pH of 2. Accordingly, maximum percentage of MB removal (97%) can be attained when the solution is at its most basic level. This explained by predominance of negative charges on the adsorbent surface at higher pH values, which increases the adhesion and electrostatic attraction of the positively charged methylene blue (MB) dye molecules (Ghouti & Absi, 2020). This result is in line with research reported by Tsade et al., (2021) on methylene blue removal from wastewater using cellulose nanomaterials. The lower percentage dye removal observed under acidic conditions attributed to adsorbent surface being positively charged in that pH environment. This positive surface charge led to electrostatic repulsion between the adsorbent and cationic methylene blue adsorbate, resulting in decreased adsorption. Percentage of removal of methylene blue dye was increased slightly from 2-6. From pH 6 to 8, the graph indicates a sharply increasing percentage of removal of the MB. After optimum value (pH = 8), the percentage of removal decreased. Figure 15(c) shows the absorbance spectrum at different pH values. The percent removal effecency and adsorption capacity were calculated according to equitions (4) and (5), respectively. Table 6 shows the percent removal and adsorption capacity at different pH changes.

Table 6: Effect of solution pH on removal efficiency and adsorption capacity of methylene blue dye

Change of pH	Removal Efficiency (% removal)	Adsorption Capacity (mg/g)
2	47.86	6.84
4	71.98	10.28
6	79.21	11.32
7	85.3	12.19
8	97.03	13.86
9	93.6	13.37
10	93.9	13.41

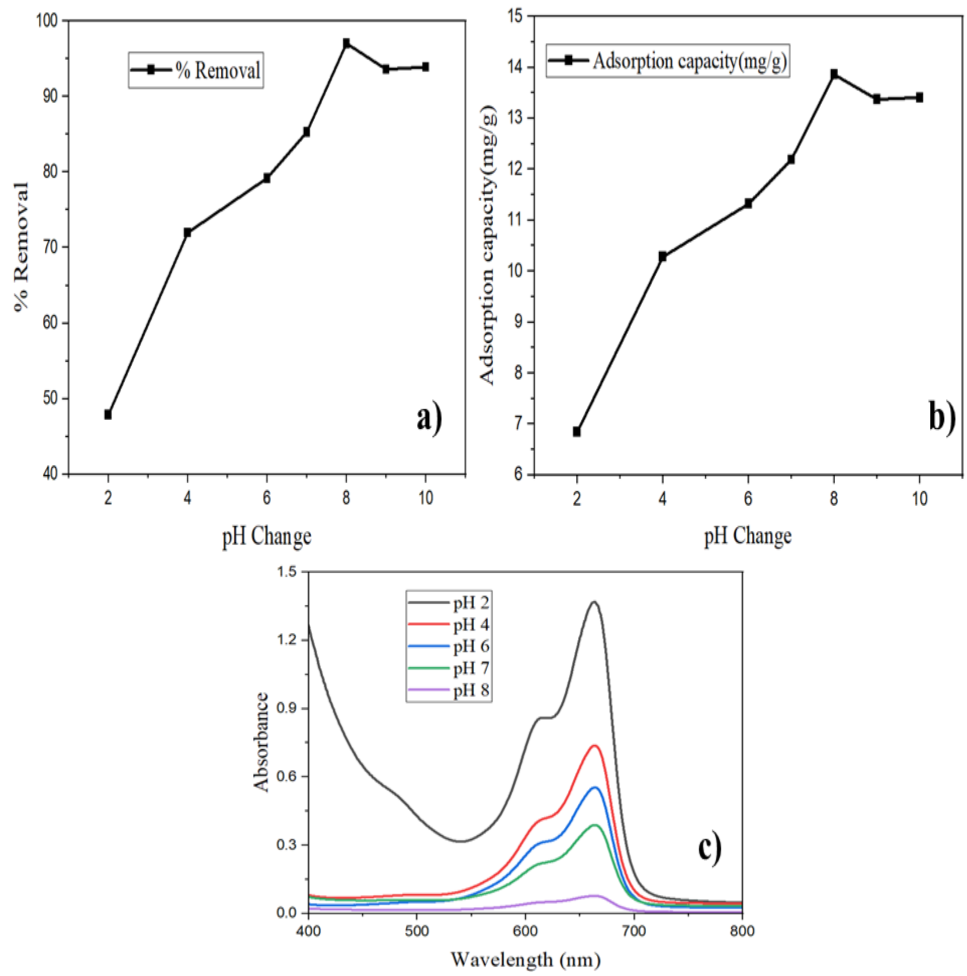

Figure 15: Effect of solution pH on methylene blue dye adsorption (a) removal efficiency (%), (b) adsorption capacity (mg/g), and (c) absorbance spectrum at different pH value (contact time = 80min, amount of sorbent 0.07g/100mL at 25^0c).

4.3.4. Effect of Initial Concentration

Effect of the initial MB concentration on adsorption efficiency and adsorption capacity of MNC adsorbent was evaluated by testing different adsorbate concentrations. Figure 16 (a and b) shows removal efficiency and adsorption capacity of MNC at different initial concentrations of the adsorbate. It is evident that the initial dye concentration is one of the key factors influencing the removal degree of the dye from the aqueous solution. As the initial methylene blue (MB) concentration was increased from 10 to 50 mg/L, the removal efficiency (shown in Figure 16a) decreased from 97% to 78.8%. The decrease in removal efficiency at higher initial dye concentrations attributed to fact that as dye concentration in the solution increases, the number of available active sites on the adsorbent surface becomes relatively scarce. This leads to a reduction in the overall degree of adsorption (Yan et al., 2014). The highest percent of adsorption was seen at 10 mg/L. The percentage removal of methylene blue (MB) dye decreases as the initial concentration of the dye in the solution increases. This observation aligns with the findings reported by Rahman et al., (2012), who also noted that the percentage removal of MB dye decreased as the concentration of MB dye in the solution was increased. Interestingly, while the percentage removal decreased with higher initial dye concentrations, the adsorbent's adsorption capacity increased, as illustrated in Figure 16b. This can be explained by the stronger mass transfer driving force that exists at the higher initial dye concentrations (Yagub et al., 2014). Figure 16(c) shows the absorbance spectra increased as the initial concentrations of adsorbate increased. The percent removal effieciency and adsorption capacity were calculated according to equitions (4) and (5), respectively. Table 7 shows the percent removal and adsorption capacity at different initial methylene blue dye concentrations.

Table 7: Effect of initial concentration on removal efficiency and adsorption capacity of methylene blue dye

Initial Concentration (mg/L)	**Adsorption Capacity (mg/g)**	**Removal Efficiency (% removal)**
10	13.85	97.03
20	24.54	85
30	33.76	83.7
40	41.29	82.5
50	59.96	78.8

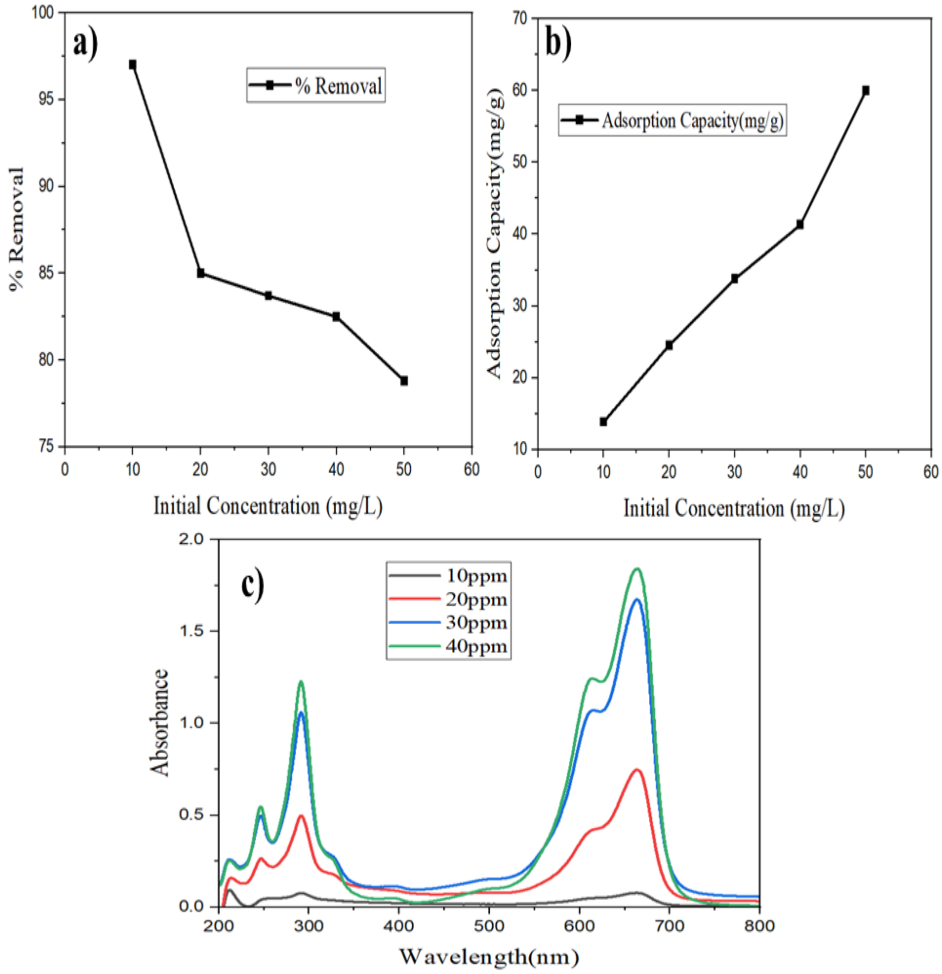

Figure 16: Initial concentration effect on methylene blue dye adsorption (a) removal efficiency (%), (b) adsorption capacity (mg/g), and (c) absorbance spectrum at different initial concentration of MB (pH = 8, contact time = 80min, amount of sorbent 0.07g/100mL at 25^0c).

4.4. Adsorption Isotherm

Figure 17(a and b) shows the Langmuir and Freundlich isotherm models. The dimensionless equilibrium parameter (RL) used to express the important characteristics of Langmuir isotherm model. This type of isotherm is identified by value of RL, which might be unfavorable (RL>1), linear (RL=1), favorable (0<RL<1), or irreversible (RL=0). The value of RL in the current study ranged from 0 to 1. The RL (the separation factor) value of 0.3694 lies between 0 and 1, which confirms that the adsorption process of MB dye was favorable on the MNC. The R^2 values of Langmuir isotherm and Freundlich were 0.996 and 0.967, respectively. According to the R^2 value, both methods were favorable in this study. However, the R^2 value of the Langmuir was greater than the R^2 value of the

Freundlich adsorption isotherm, for this reason, the Langmuir isotherm model fits better than the Fredundlich isotherm model. The maximum adsorption capacity of MNC was reported at 102.35 mg/g. Tables 8 and 9 show Langmuir and Freundlich adsorption isotherm parameters, respectively.

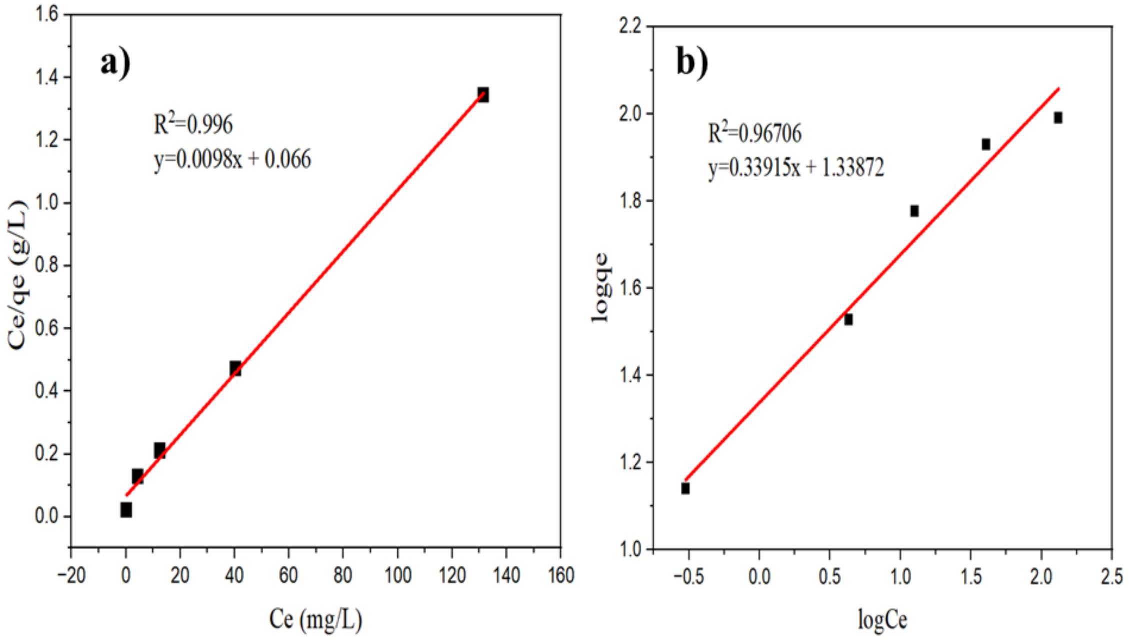

Figure 17: Plot of adsorption isotherm model a) Langmuir adsorption isotherm model, and b) Freundlich adsorption isotherm model at different initial concentration of methylene blue dye (10-200 mg/L), (pH = 8, contact time = 80min, amount of sorbent 0.07g/100mL at 25^0c).

Table 8: Langmuir adsorption isotherm parameters

Intercept	**Slope**	**Qmax**	**K_L**	**R_L**	**R^2**
0.06614	0.00977	102.35	0.01414	0.3694	0.99615

Table 9: Freundlich adsorption isotherm parameters

Intercept	**Slope**	**n**	**1/n**	**Kf**	**R^2**
1.33872	0.33915	2.948548	0.33915	21.8132	0.97

4.5. Adsorption Kinetics

As illustrated in Figure 18a, the R^2 value for the pseudo second order kinetic model is very close to 1. This model provides a higher value of qe (30.22 mg/g) than pseudo first order kinetic model (23.56 mg/g). Based on the R^2 values, the adsorption of the cationic methylene blue (MB) dye onto MNC adsorbent fits well with the pseudo second order kinetic model. Previous investigation have also reported by Kara et al., (2021), that uptake of MB dye on cellulose based adsorbents was a pseudo second order kinetic model, it is consistent with findings for the MNC adsorbent in this study. As shown in Figure 18b, the pseudo second order kinetic model with an R^2 = 0.996 fits experimental data better than pseudo first order kinetic model, which had lower R^2 = 0.83. Pseudo second order model applies to external liquid membrane diffusion, surface adsorption, and intra-particle diffusion, implying that chemical adsorption influences the adsorption process by involving electron exchange or sharing between MB cations and functional groups on the biomass surface. Generally, adsorption of methylene blue dye onto MNC adsorbent well stated by pseudo second order kinetic. This suggests that the adsorption of methylene blue dye onto MNC characterized as a chemical adsorption process. Kinetic data for adsorption of methylene blue onto the MNC adsorbent is summarized in Table 10. This includes pseudo first order and pseudo second order kinetic models, also an experimentally determined equilibrium adsorption capacity (qe_{ex}) of 29.33 mg/g.

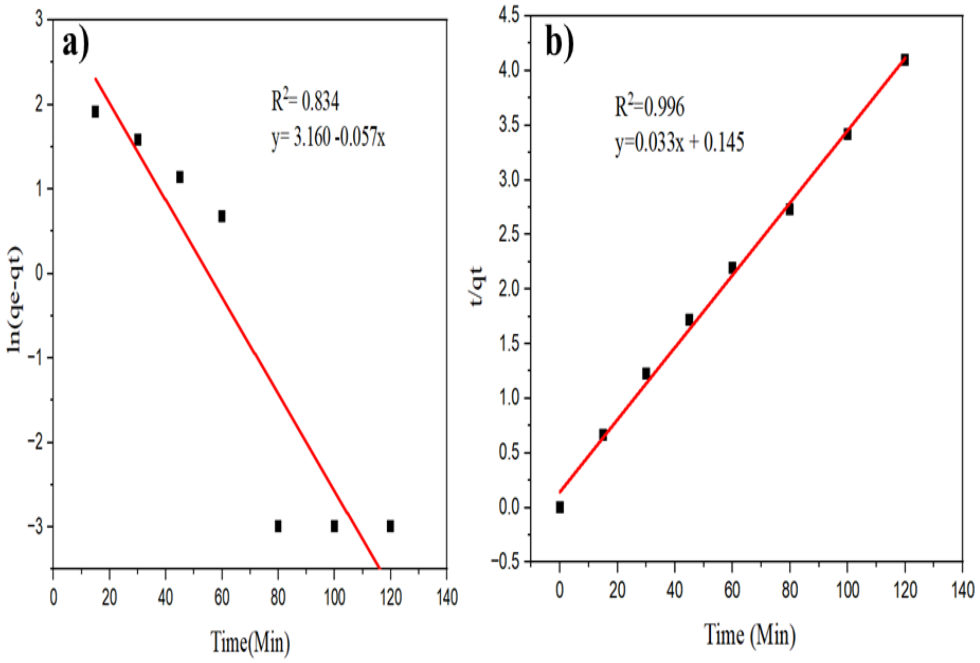

Figure 18: curve of adsorption kinetics parameters pesudo frist order (a), and pseudo second order (b).

Table 10: Adosrption kinetics parameters for pesudo second order and pesudo frist order

Pseudo Second Order	**Intercept**	**Slope**	**qe_{cal}(mg/g)**	**qe^2**	**K_2**	**R^2**
	0.14472	0.03309	30.22061	913.2853	0.007566	0.99604
Pseudo Frist Order	**Intercept**	**Slope**	**qe_{cal}(mg/g)**		**K_1**	**R^2**
	3.15962	-0.0573	23.56164		-0.00072	0.834

4.6. Reusability Study

Reusability of the adsorbent is a useful factor to be considered when evaluating the practical applicability of the adsorbent for treatment of aqueous solutions. Figure (19a) shows the removal efficiency of regenerate MNC, the efficiency of adsorbent dropped from 97 % to 88.97 % after 5 consecutive usages. Figure (19b) shows the collecting of MNC using an external magnetite in recycling process of the prepared materials. Overall, it can be concluded that MNC has good regeneration and reusability potential. Table 11 provides information about the removal efficiency of MB by MNC adsorbent after different cycles of use.

Table 11: Removal efficiency of methylene blue dye after different cycles

No of Recycle	Absorbance	% Removal
1	0.078	97
2	0.132	95.2
3	0.233	91.04
4	0.26	90.1
5	0.312	88.97

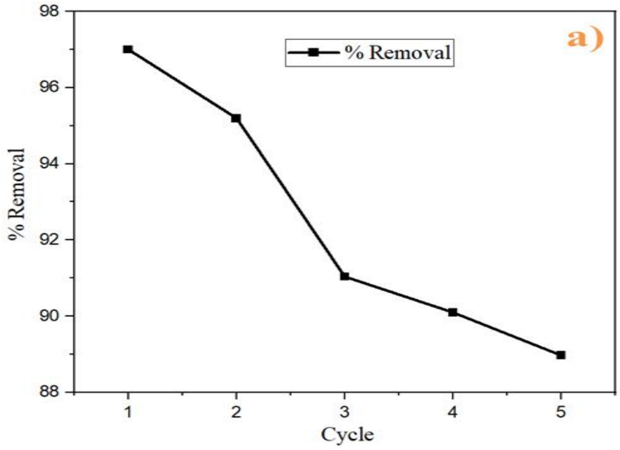

Figure 19: Reusability of MNC removal efficiency (a), and collect MNC by external magnetite (b) at adsorbent dosage 0.07 g, pH=8, time 80 min, and MB dye concentration = 10 mg/L.

5. CONCLUSION

This study was concentrated on synthesis of magnetite Impregnated nanocellulose composites (MNC) composites using khat stem biomass as the source material. The objective was to utilize these MNC composites for the elimination of methylene blue dye from aqueous solutions. The MNC was synthesized via the co-precipitation method. The prepared materials were characterized using DSC, XRD, FTIR, SEM, and BET surface area analysis. The DSC result showed that MNC was more thermally stable than nanocellulose (NC). The basic functional groups of prepared materials have been identified by FTIR spectroscopy. Average crystallite size of MNC was 8.02 nm. The BET multi point surface area, NLDFT cumulative surface area, average pore size, and total pore volume of MNC were 511.735 m^2/g, 154.1 m^2/g, 0.619 nm, and 1.335 cc/g, respectively, which indicate that the MNC is best for the adsorption of MB dye. This study explored the influence of various experimental factors including pH, initial adsorbate concentration contact time, and adsorbent dose, in order to identify the optimum parameter values for the adsorption process. The results showed that varying these experimental factors had an impact on the adsorption process. The study found that maximum adsorption efficiency of 97% achieved under the following optimum conditions: pH 8, 80 minutes contact time, 10 mg/L methylene blue dye concentration, and 0.07 g/100mL of MNC adsorbent dose, all at room temperature. Kinetic data analysis indicates pseudo second order kinetic model provided a more fit to experimental data, with a higher $R^2 = 0.996$ compared to pseudo first order model, this suggests that better described by a chemisorption mechanism. Langmuir isotherm model was more fitted in this study than Freundlich isotherm model, its R^2 and maximum adsorption capacity was 0.996 and 102.35 mg/g, respectively. The Khat stem based magnetite impregnated nanocellulose composite was effective during the recyclability test. According to the reusability test, MNC can remove methylene blue dye at a rate of 97 to 88.97 % from cycle 1 to cycle 5. These and previous results show that Khat stem based magnetite impregnated nanocellulose composites could potentially remove MB dye from aqueous solutions.

6. RECOMMENDATIONS

Previous research has investigated various alternative adsorbents for removal of methylene blue dye from water. There are already thousands of adsorbent options available, ranging from low-cost agricultural waste to sophisticated compounds like carbon nanotubes. However, none of these materials are currently used in industry, and more research is needed to develop these types of materials as industrial adsorbent. Numerous variables must be examined before these alternative adsorbents will be developed as commercial adsorbents to removal MB from water. Adsorption studies should be conducted on real water (wastewater). In future investigations, recovering MB after recycling process will be the best and most cost effective way.

RESEARCH FUND ACKNOWLEDGMENT

This research was funded by Adama Science and Technology University under grant number ASTU/ SM-R /1001/24.

REFERENCES

Abd-Elhamid, A. I., Emran, M., El-Sadek, M. H., El-Shanshory, A. A., Soliman, H. M. A., Akl, M. A., & Rashad, M. (2020). Enhanced removal of cationic dye by eco-friendly activated biochar derived from rice straw. *Applied Water Science*, *10*(1), 45. https://doi.org/10.1007/s13201-019-1128-0

Abdelrahman, E. A., Hegazey, R. M., & El-Azabawy, R. E. (2019). Efficient removal of methylene blue dye from aqueous media using Fe/Si, Cr/Si, Ni/Si, and Zn/Si amorphous novel adsorbents. *Journal of Materials Research and Technology*, *8*(6), 5301–5313. https://doi.org/10.1016/j.jmrt.2019.08.051

Abolore, R. S., Jaiswal, S., & Jaiswal, A. K. (2024). Green and sustainable pretreatment methods for cellulose extraction from lignocellulosic biomass and its applications: A review. *Carbohydrate Polymer Technologies and Applications*, *7*(November 2023), 100396. https://doi.org/10.1016/j.carpta.2023.100396

Aklillu, E., & Engidawork, E. (2021). The impact of catha edulis (vahl) forssk. ex endl. (celestraceae) (khat) on pharmacokinetics of clinically used drugs. *Expert Opinion on Drug Metabolism and Toxicology*, *17*(9), 1125–1138. https://doi.org/10.1080/17425255.2021.1971194

Akperov, E. O., & Akperov, O. H. (2019). The wastage of the cotton stalks (Gossypium hirsutum L.) as low-cost adsorbent for removal of the Basic Green 5 dye from aqueous solutions. *Applied Water Science*, *9*(8), 183. https://doi.org/10.1007/s13201-019-1071-0

Al-Degs, Y., Khraisheh, M. A. M., Allen, S. J., Ahmad, M. N., & Walker, G. M. (2007). Competitive adsorption of reactive dyes from solution: Equilibrium isotherm studies in single and multisolute systems. *Chemical Engineering Journal*, *128*(2–3), 163–167. https://doi.org/10.1016/j.cej.2006.10.009

Ali, A., Zafar, H., Zia, M., ul Haq, I., Phull, A. R., Ali, J. S., & Hussain, A. (2016). Synthesis, characterization, applications, and challenges of iron oxide nanoparticles. *Nanotechnology, Science and Applications*, *Volume 9*, 49–67. https://doi.org/10.2147/NSA.S99986

Amiralian, N., Mustapic, M., Hossain, M. S. A., Wang, C., Konarova, M., Tang, J., Na, J., Khan, A., & Rowan, A. (2020). Magnetic nanocellulose: A potential material for removal of dye from water. *Journal of Hazardous Materials*, *394*(February), 122571. https://doi.org/10.1016/j.jhazmat.2020.122571

Amran, M., Salleh, M., Khalid, D., Azlina, W., Abdul, W., & Idris, A. (2011). *Cationic and anionic dye adsorption by agricultural solid wastes : A comprehensive review*. *280*, 1–13. https://doi.org/10.1016/j.desal.2011.07.019

Arevalo-Gallegos, A., Ahmad, Z., Asgher, M., Parra-Saldivar, R., & Iqbal, H. M. N. (2017). Lignocellulose: A sustainable material to produce value-added products with a zero waste approach-A review. *International Journal of Biological Macromolecules*, *99*, 308–318. https://doi.org/10.1016/j.ijbiomac.2017.02.097

Assonfack, H. L., Yona Cheumani, A. M., Ndinteh, D., Lembe, J. T., Nga, J. B., & Ndikontar, M. K. (2023). Preparation and Characterisation of Cellulose by Delignification of Eteng (Ceiba pentandra) Wood in Formic Acid-Acetic Acid-Water Solvent Mixtures. *Journal of Polymers and the Environment*, *31*(3), 913–921. https://doi.org/10.1007/s10924-022-02641-9

Baabu, P. R. S., Kumar, H. K., Gumpu, M. B., Babu K, J., Kulandaisamy, A. J., & Rayappan, J. B. B. (2022). Iron Oxide Nanoparticles: A Review on the Province of Its Compounds, Properties and Biological Applications. *Materials*, *16*(1), 59. https://doi.org/10.3390/ma16010059

Bănăduc, D., Simić, V., Cianfaglione, K., Barinova, S., Afanasyev, S., Öktener, A., McCall, G., Simić, S., & Curtean-Bănăduc, A. (2022). Freshwater as a Sustainable Resource and Generator of Secondary Resources in the 21st Century: Stressors, Threats, Risks, Management and Protection Strategies, and Conservation Approaches. *International Journal of Environmental Research and Public Health*, *19*(24), 16570. https://doi.org/10.3390/ijerph192416570

Batmaz, R., Mohammed, N., Zaman, M., Minhas, G., Berry, R. M., & Tam, K. C. (2014). Cellulose nanocrystals as promising adsorbents for the removal of cationic dyes. *Cellulose*, *21*(3), 1655–1665. https://doi.org/10.1007/s10570-014-0168-8

Bedada, W., de Andrés, F., Engidawork, E., Hussein, J., LLerena, A., & Aklillu, E. (2018).

Effects of Khat (Catha edulis) use on catalytic activities of major drug-metabolizing cytochrome P450 enzymes and implication of pharmacogenetic variations. *Scientific Reports*, *8*(1), 12726. https://doi.org/10.1038/s41598-018-31191-1

Berger, A. H., & Bhown, A. S. (2011). Comparing physisorption and chemisorption solid sorbents for use separating CO2 from flue gas using temperature swing adsorption. *Energy Procedia*, *4*, 562–567. https://doi.org/10.1016/j.egypro.2011.01.089

Brinchi, L., Cotana, F., Fortunati, E., & Kenny, J. M. (2013). Production of nanocrystalline cellulose from lignocellulosic biomass: technology and applications. *Carbohydrate Polymers*, *94*(1), 154–169. https://doi.org/10.1016/j.carbpol.2013.01.033

Brodeur, G., Yau, E., Badal, K., Collier, J., Ramachandran, K. B., & Ramakrishnan, S. (2011). Chemical and Physicochemical Pretreatment of Lignocellulosic Biomass: A Review. *Enzyme Research*, *2011*(1), 1–17. https://doi.org/10.4061/2011/787532

Chakraborty, B., Ray, L., & Basu, S. (2016). Biochemical degradation of Methylene Blue using a continuous reactor packed with solid waste by E. coli and Bacillus subtilis isolated from wetland soil. *Desalination and Water Treatment*, *57*(30), 14077–14082. https://doi.org/10.1080/19443994.2015.1063089

Chan, C. H., Chia, C. H., Zakaria, S., Sajab, M. S., & Chin, S. X. (2015). Cellulose nanofibrils: a rapid adsorbent for the removal of methylene blue. *RSC Advances*, *5*(24), 18204–18212. https://doi.org/10.1039/C4RA15754K

Collivignarelli, M. C., Abbà, A., Carnevale Miino, M., & Damiani, S. (2019). Treatments for color removal from wastewater: State of the art. *Journal of Environmental Management*, *236*, 727–745. https://doi.org/10.1016/j.jenvman.2018.11.094

Cova, T. F., Murtinho, D., Aguado, R., Pais, A. A. C. C., & Valente, A. J. M. (2021). Cyclodextrin Polymers and Cyclodextrin-Containing Polysaccharides for Water Remediation. *Polysaccharides*, *2*(1), 16–38. https://doi.org/10.3390/polysaccharides2010002

Crini, G., & Lichtfouse, E. (2019). Advantages and disadvantages of techniques used for wastewater treatment. *Environmental Chemistry Letters*, *17*(1), 145–155. https://doi.org/10.1007/s10311-018-0785-9

Daifullah, A. A. M., Girgis, B. S., & Gad, H. M. H. (2003). Utilization of agro-residues (rice husk) in small waste water treatment plans. *Materials Letters*, *57*(11), 1723–1731. https://doi.org/10.1016/S0167-577X(02)01058-3

Darcheville, M. (2021). *magnetic coatings by fluid processing Synthesis of iron oxide nanoparticles and development of magnetic coatings by fluid processing par Thèse de doctorat*.

Demesa, A. G., Laari, A., & Sillanpää, M. (2020). Value-added chemicals and materials from lignocellulosic biomass. In *Advanced Water Treatment* (pp. 367–436). Elsevier. https://doi.org/10.1016/B978-0-12-819225-2.00006-5

Derakhshan, Z., Baghapour, M. A., & Ranjbar, M. (2013). *h c v i o e h c v i o e f*. *2*(3).

Dufresne, A. (2019). Nanocellulose Processing Properties and Potential Applications. *Current Forestry Reports*, *5*(2), 76–89. https://doi.org/10.1007/s40725-019-00088-1

Ebi Ebi, O., Falilat Taiwo, A., & Tunde Folorunsho, A. (2018). Kinetic Modelling of the Biosorption of Methylene Blue onto Wild Melon (Lagenariasphaerica). *American Journal of Chemical Engineering*, *6*(6), 126–134. https://doi.org/10.11648/j.ajche.20180606.12

El-Gendy, N. S., & Nassar, H. N. (2021). Biosynthesized magnetite nanoparticles as an environmental opulence and sustainable wastewater treatment. *Science of The Total Environment*, *774*, 145610. https://doi.org/10.1016/j.scitotenv.2021.145610

El-Nahas, A. M., Salaheldin, T. A., Zaki, T., El-Maghrabi, H. H., Marie, A. M., Morsy, S. M., & Allam, N. K. (2017). Functionalized cellulose-magnetite nanocomposite catalysts for efficient biodiesel production. *Chemical Engineering Journal*, *322*, 167–180. https://doi.org/10.1016/j.cej.2017.04.031

Evans, S. K., Wesley, O. N., Koech, L., Nelana, S. M., & Rutto, H. L. (2022). Structural Features of Cellulose and Cellulose Nanocrystals via In Situ Incorporation of Magnetic Iron Oxide Nanoparticles: Modification and Characterization. *Coatings*, *13*(1), 39. https://doi.org/10.3390/coatings13010039

Fatahi, H., Claverie, J., & Poncet, S. (2022). Thermal Characterization of Phase Change Materials by Differential Scanning Calorimetry: A Review. *Applied Sciences*, *12*(23), 12019. https://doi.org/10.3390/app122312019

Fong, W. M., Affam, A. C., & Chung, W. C. (2020). Synthesis of Ag/Fe/CAC for colour and COD removal from methylene blue dye wastewater. *International Journal of Environmental Science and Technology*, *17*(7), 3485–3494. https://doi.org/10.1007/s13762-020-02720-1

Gabriel, T., Wondu, K., & Dilebo, J. (2021). Valorization of khat (Catha edulis) waste for the production of cellulose fibers and nanocrystals. *PLOS ONE*, *16*(2), e0246794. https://doi.org/10.1371/journal.pone.0246794

Gao, J., Qin, Y., Zhou, T., & Cao, D. (2013). *Adsorption of methylene blue onto activated carbon produced from tea (Camellia sinensis L .) seed shells : kinetics , equilibrium , and thermodynamics studies **. *14*(7), 650–658. https://doi.org/10.1631/jzus.B12a0225

Gayathri, P., Senthil Kumar, A., & Kamaraj, S. (2015). An Unusual Electrochemical Reductive Cleavage of Azo Dye into Highly Redox Active Copolymeric Aniline Derivatives on a MWCNT Modified Electrode Surface at Neutral pH and Its Electroanalytical Features. *The Journal of Physical Chemistry C*, *119*(14), 7791–7801. https://doi.org/10.1021/acs.jpcc.5b00612

Gebissa, E. (2010). Khat in the Horn of Africa: Historical perspectives and current trends. *Journal of Ethnopharmacology*, *132*(3), 607–614. https://doi.org/10.1016/j.jep.2010.01.063

Gessesse Dessie. (2013). *Favouring a Demonised Plant Khat and Ethiopian smallholder-enterprises*. *51*, 29. http://www.diva-portal.org/smash/record.jsf?pid=diva2:586499

Getasetegn, M. (2016). Chemical composition of Catha edulis (khat): a review. *Phytochemistry Reviews*, *15*(5), 907–920. https://doi.org/10.1007/s11101-015-9435-z

Ghouti, M. A. Al, & Absi, R. S. Al. (2020). *Mechanistic understanding of the adsorption and thermodynamic aspects of cationic methylene blue dye onto cellulosic olive stones biomass from wastewater*. 1–18.

Gupta, V. K., & Suhas. (2009). Application of low-cost adsorbents for dye removal--a review. *Journal of Environmental Management*, *90*(8), 2313–2342.

https://doi.org/10.1016/j.jenvman.2008.11.017

Hameed, B. H., Din, A. T. M., & Ahmad, A. L. (2007). *Adsorption of methylene blue onto bamboo-based activated carbon : Kinetics and equilibrium studies*. *141*, 819–825. https://doi.org/10.1016/j.jhazmat.2006.07.049

Handayani, T., Emriadi, Deswati, Ramadhani, P., & Zein, R. (2024). Modelling studies of methylene blue dye removal using activated corn husk waste: Isotherm, kinetic and thermodynamic evaluation. *South African Journal of Chemical Engineering*, *47*(October 2023), 15–27. https://doi.org/10.1016/j.sajce.2023.10.003

Hassan Rashid, M. A. U., Manzoor, M. M., & Mukhtar, S. (2018). Urbanization and Its Effects on Water Resources: An Exploratory Analysis. *Asian Journal of Water, Environment and Pollution*, *15*(1), 67–74. https://doi.org/10.3233/AJW-180007

Hokkanen, S., & Sillanpää, M. (2020). Nano- and microcellulose-based adsorption materials in water treatment. In *Advanced Water Treatment* (pp. 1–83). Elsevier. https://doi.org/10.1016/B978-0-12-819216-0.00001-1

Holkar, C. R., Jadhav, A. J., Pinjari, D. V., Mahamuni, N. M., & Pandit, A. B. (2016). A critical review on textile wastewater treatments: Possible approaches. *Journal of Environmental Management*, *182*, 351–366. https://doi.org/10.1016/j.jenvman.2016.07.090

Huang, D., Li, R., Xu, P., Li, T., Deng, R., Chen, S., & Zhang, Q. (2020). The cornerstone of realizing lignin value-addition: Exploiting the native structure and properties of lignin by extraction methods. *Chemical Engineering Journal*, *402*, 126237. https://doi.org/10.1016/j.cej.2020.126237

Ismail, M., Akhtar, K., Khan, M. I., Kamal, T., Khan, M. A., M. Asiri, A., Seo, J., & Khan, S. B. (2019). Pollution, Toxicity and Carcinogenicity of Organic Dyes and their Catalytic Bio-Remediation. *Current Pharmaceutical Design*, *25*(34), 3645–3663. https://doi.org/10.2174/1381612825666191021142026

Jaishankar, M., Tseten, T., Anbalagan, N., Mathew, B. B., & Beeregowda, K. N. (2014). *Toxicity , mechanism and health effects of some heavy metals*. *7*(2), 60–72. https://doi.org/10.2478/intox-2014-0009

Jodeh, S., Hamed, O., Melhem, A., Salghi, R., Jodeh, D., Azzaoui, K., Benmassaoud, Y., & Murtada, K. (2018). Magnetic nanocellulose from olive industry solid waste for the effective removal of methylene blue from wastewater. *Environmental Science and Pollution Research International*, *25*(22), 22060–22074. https://doi.org/10.1007/s11356-018-2107-y

John, M. (2017). *Impact of Iron Oxide Nanoparticles on the Anaerobic Digestion Process*. *May 2024*.

Jonoobi, M., Oladi, R., Davoudpour, Y., Oksman, K., Dufresne, A., Hamzeh, Y., & Davoodi, R. (2015). Different preparation methods and properties of nanostructured cellulose from various natural resources and residues: a review. *Cellulose*, *22*(2), 935–969. https://doi.org/10.1007/s10570-015-0551-0

Jorfi, M., & Foster, E. J. (2015). Recent advances in nanocellulose for biomedical applications. *Journal of Applied Polymer Science*, *132*(14), 1–19. https://doi.org/10.1002/app.41719

Kalogeras, I. M., & Hagg Lobland, H. E. (2012). The nature of the glassy state: Structure and glass transitions. *Journal of Materials Education*, *34*(3–4), 69–94.

Kamaraj, M., Srinivasan, N. R., Assefa, G., & Adugna, A. T. (2020). Environmental Technology & Innovation Facile development of sunlit ZnO nanoparticles-activated carbon hybrid from pernicious weed as an operative nano-adsorbent for removal of methylene blue and chromium from aqueous solution : Extended application in tan. *Environmental Technology & Innovation*, *17*, 100540. https://doi.org/10.1016/j.eti.2019.100540

Kanmani, P., Aravind, J., Kamaraj, M., Sureshbabu, P., & Karthikeyan, S. (2017). Environmental applications of chitosan and cellulosic biopolymers: A comprehensive outlook. *Bioresource Technology*, *242*, 295–303. https://doi.org/10.1016/j.biortech.2017.03.119

Kara, H. T., Anshebo, S. T., & Sabir, F. K. (2021). *Adsorptive Removal of Cd (II) Ions from Wastewater Using Maleic Anhydride Nanocellulose*. *2021*(Ii).

Kara, H. T., Anshebo, S. T., Sabir, F. K., & Workineh, G. A. (2021). *Removal of Methylene Blue Dye from Wastewater Using Periodiated Modified Nanocellulose*.

2021.

Katheresan, V., Kansedo, J., & Lau, S. Y. (2018). Efficiency of various recent wastewater dye removal methods: A review. *Journal of Environmental Chemical Engineering*, *6*(4), 4676–4697. https://doi.org/10.1016/j.jece.2018.06.060

Khaled, A., Nemr, A. El, El-Sikaily, A., & Abdelwahab, O. (2009). Removal of Direct N Blue-106 from artificial textile dye effluent using activated carbon from orange peel: Adsorption isotherm and kinetic studies. *Journal of Hazardous Materials*, *165*(1–3), 100–110. https://doi.org/10.1016/j.jhazmat.2008.09.122

Khan, I., Saeed, K., Zekker, I., Zhang, B., Hendi, A. H., Ahmad, A., Ahmad, S., Zada, N., Ahmad, H., Shah, L. A., Shah, T., & Khan, I. (2022). Review on Methylene Blue: Its Properties, Uses, Toxicity and Photodegradation. *Water*, *14*(2), 242. https://doi.org/10.3390/w14020242

Kim, J. S., Lee, Y. Y., & Kim, T. H. (2016). A review on alkaline pretreatment technology for bioconversion of lignocellulosic biomass. *Bioresource Technology*, *199*, 42–48. https://doi.org/10.1016/j.biortech.2015.08.085

Kim, W., Suh, C.-Y., Cho, S.-W., Roh, K.-M., Kwon, H., Song, K., & Shon, I.-J. (2012). A new method for the identification and quantification of magnetite–maghemite mixture using conventional X-ray diffraction technique. *Talanta*, *94*, 348–352. https://doi.org/10.1016/j.talanta.2012.03.001

Klemm, D., Heublein, B., Fink, H., & Bohn, A. (2005). Cellulose: Fascinating Biopolymer and Sustainable Raw Material. *Angewandte Chemie International Edition*, *44*(22), 3358–3393. https://doi.org/10.1002/anie.200460587

Ko, J. K., Bak, J. S., Jung, M. W., Lee, H. J., Choi, I.-G., Kim, T. H., & Kim, K. H. (2009). Ethanol production from rice straw using optimized aqueous-ammonia soaking pretreatment and simultaneous saccharification and fermentation processes. *Bioresource Technology*, *100*(19), 4374–4380. https://doi.org/10.1016/j.biortech.2009.04.026

Kumar, A., Sood, A., & Soo Han, S. (2021). Potential of magnetic nano cellulose in biomedical applications: Recent Advances. *Biomaterials and Polymers Horizon*, *1*(1), 32–47. https://doi.org/10.37819/bph.001.01.0133

Li, C., & Knierim, B. (2010). *DigitalCommons @ University of Nebraska - Lincoln Comparison of dilute acid and ionic liquid pretreatment of switchgrass : Biomass recalcitrance , delignification and enzymatic saccharification*.

Lingegowda, D. C., Kumar, J. K., Prasad, A. G. D., Zarei, M., & Gopal, S. (2013). Ftir Spectroscopic Studies on Cleome Gynandra – Comparative ANALYSIS OF FUNCTIONAL GROUP BEFORE AND AFTER EXTRACTION. *Romanian Journal of Biophysics*, *22*(June 2014), 137–143.

Lo Faro, A. F., Di Trana, A., La Maida, N., Tagliabracci, A., Giorgetti, R., & Busardò, F. P. (2020). Biomedical analysis of New Psychoactive Substances (NPS) of natural origin. *Journal of Pharmaceutical and Biomedical Analysis*, *179*, 112945. https://doi.org/10.1016/j.jpba.2019.112945

Mashkoor, F., & Nasar, A. (2020). Magsorbents: Potential candidates in wastewater treatment technology – A review on the removal of methylene blue dye. *Journal of Magnetism and Magnetic Materials*, *500*, 166408. https://doi.org/10.1016/j.jmmm.2020.166408

Melhem, A. M. R. (2017). *Synthesis and characterization of magnetic nano cellulose from olive waste (Jeft) for the effective removal of methylene blue from water*. https://repository.najah.edu/handle/20.500.11888/13177%0Ahttps://repository.najah.edu/bitstream/handle/20.500.11888/13177/ 1.pdf?sequence=1

Mishra, R. K., Sabu, A., & Tiwari, S. K. (2018). Materials chemistry and the futurist eco-friendly applications of nanocellulose: Status and prospect. *Journal of Saudi Chemical Society*, *22*(8), 949–978. https://doi.org/10.1016/j.jscs.2018.02.005

Mohan, V. B., Jayaraman, K., & Bhattacharyya, D. (2020). Brunauer–Emmett–Teller (BET) specific surface area analysis of different graphene materials: A comparison to their structural regularity and electrical properties. *Solid State Communications*, *320*, 114004. https://doi.org/10.1016/j.ssc.2020.114004

Mokaloba, N., & Batane, R. (2014). The effects of mercerization and acetylation treatments on the properties of sisal fiber and its interfacial adhesion characteristics on polypropylene. *International Journal of Engineering, Science and Technology*, *6*(4), 83. https://doi.org/10.4314/ijest.v6i4.9

Mondal, S., De Anda Reyes, M. E., & Pal, U. (2017). Plasmon induced enhanced photocatalytic activity of gold loaded hydroxyapatite nanoparticles for methylene blue degradation under visible light. *RSC Advances*, *7*(14), 8633–8645. https://doi.org/10.1039/C6RA28640B

Moussout, H., Ahlafi, H., Aazza, M., & Maghat, H. (2018). Critical of linear and nonlinear equations of pseudo-first order and pseudo-second order kinetic models. *Karbala International Journal of Modern Science*, *4*(2), 244–254. https://doi.org/10.1016/j.kijoms.2018.04.001

Muswareen, S. K. K., Venkatarao, K., & Cole, S. (2023). Comparative Study of Crystallite Size from XRD and TEM Results for Pure and V2O5 Doped CdO-FePO4 Composite Nanopowders. *Physical Chemistry Research*, *11*(2), 241–251. https://doi.org/10.22036/PCR.2022.337333.2077

Nam, S., French, A. D., Condon, B. D., & Concha, M. (2016). Segal crystallinity index revisited by the simulation of X-ray diffraction patterns of cotton cellulose Iβ and cellulose II. *Carbohydrate Polymers*, *135*, 1–9. https://doi.org/10.1016/j.carbpol.2015.08.035

Nasr, J. Ben, Hamdi, N., & Elhalouani, F. (2017). Characterization of activated carbon Prepared from sludge paper for methylene blue adsorption. *Journal of Materials and Environmental Science*, *8*(6), 1960–1967.

Nebaghe, K. C., El Boundati, Y., Ziat, K., Naji, A., Rghioui, L., & Saidi, M. (2016). Comparison of linear and non-linear method for determination of optimum equilibrium isotherm for adsorption of copper(II) onto treated Martil sand. *Fluid Phase Equilibria*, *430*, 188–194. https://doi.org/10.1016/j.fluid.2016.10.003

Nichols, T., Khondkar, P., & Gibbons, S. (2015). The psychostimulant drug khat (Catha edulis): A mini-review. *Phytochemistry Letters*, *13*, 127–133. https://doi.org/10.1016/j.phytol.2015.05.016

Nurbas, M., Ghorbanpoor, H., & Avci, H. (2017). An eco-friendly approach to synthesis and characterization of magnetite (Fe3O4) nanoparticles using Platanus Orientalis L. leaf extract. *Digest Journal of Nanomaterials and Biostructures*, *12*(4), 993–1000.

Nypelö, T. (2022). Magnetic cellulose: does extending cellulose versatility with magnetic functionality facilitate its use in devices? *Journal of Materials Chemistry C*, *10*(3), 805–818. https://doi.org/10.1039/D1TC02105B

Olani, A. B., Gerbaba, M., Getnet, M., Soboka, M., & Decorte, T. (2023). Is chewing khat associated with mental health disorders? A scoping review of the content and quality of the current evidence base. *Substance Abuse Treatment, Prevention, and Policy*, *18*(1), 39. https://doi.org/10.1186/s13011-023-00545-y

Olsson, C., & Westm, G. (2013). Cellulose is a linear biohomopolymer of β-D-glucopyranose units that are linked by β-glucosidic bonds (β 1–4) and intramolecular interactions generated between adjacent cellulose units. Each glucose unit contains six carbons and three hydroxyl groups. The. In *Cellulose - Fundamental Aspects*. InTech. https://doi.org/10.5772/52144

Omran, A. A. B., Mohammed, A. A. B. A., Sapuan, S. M., Ilyas, R. A., Asyraf, M. R. M., Rahimian Koloor, S. S., & Petrů, M. (2021). Micro- and Nanocellulose in Polymer Composite Materials: A Review. *Polymers*, *13*(2), 231. https://doi.org/10.3390/polym13020231

Pandey, S., Do, J. Y., Kim, J., & Kang, M. (2020). Fast and highly efficient removal of dye from aqueous solution using natural locust bean gum based hydrogels as adsorbent. *International Journal of Biological Macromolecules*, *143*, 60–75. https://doi.org/10.1016/j.ijbiomac.2019.12.002

Peter, S., Lyczko, N., Gopakumar, D., Maria, H. J., Nzihou, A., & Thomas, S. (2022). Nanocellulose and its derivative materials for energy and environmental applications. *Journal of Materials Science*, *57*(13), 6835–6880. https://doi.org/10.1007/s10853-022-07070-6

Pham, V. L., Kim, D.-G., & Ko, S.-O. (2020). Mechanisms of Methylene Blue Degradation by Nano-Sized β-MnO2 Particles. *KSCE Journal of Civil Engineering*, *24*(5), 1385–1394. https://doi.org/10.1007/s12205-020-2036-4

Phanthong, P., Reubroycharoen, N. E. and application P., Hao, X., Xu, G., Abudula, A., & Guan, G. (2018). Nanocellulose: Extraction and application. *Carbon Resources Conversion*, *1*(1), 32–43. https://doi.org/10.1016/j.crcon.2018.05.004

Rahman, M. A., Amin, S. M. R., & Alam, A. M. S. (2012). Removal of Methylene Blue from Waste Water Using Activated Carbon Prepared from Rice Husk. *Dhaka University Journal of Science*, *60*(2), 185–189. https://doi.org/10.3329/dujs.v60i2.11491

Rameshwar, H. Y., & Argaw, A. (2016). Manurial value of khat waste vermicompost from Awday, Harar town, Ethiopia. *International Journal of Recycling of Organic Waste in Agriculture*, *5*(2), 105–111. https://doi.org/10.1007/s40093-016-0121-y

Rashid, R., Shafiq, I., Akhter, P., Iqbal, M. J., & Hussain, M. (2021). A state-of-the-art review on wastewater treatment techniques: the effectiveness of adsorption method. *Environmental Science and Pollution Research International*, *28*(8), 9050–9066. https://doi.org/10.1007/s11356-021-12395-x

Rashid, S., & Dutta, H. (2020). Industrial Crops & Products Characterization of nanocellulose extracted from short , medium and long grain rice husks. *Industrial Crops & Products*, *154*(July 2019), 112627. https://doi.org/10.1016/j.indcrop.2020.112627

Rathi, B. S., Kumar, P. S., & Vo, D.-V. N. (2021). Critical review on hazardous pollutants in water environment: Occurrence, monitoring, fate, removal technologies and risk assessment. *The Science of the Total Environment*, *797*, 149134. https://doi.org/10.1016/j.scitotenv.2021.149134

Reddy, K. O., Maheswari, C. U., & Shukla, M. (2013). *Physico-Chemical Characterization of Cellulose Extracted from Ficus Leaves*. *7*(4), 496–499. https://doi.org/10.1166/jbmb.2013.1342

Revellame, E. D., Fortela, D. L., Sharp, W., Hernandez, R., & Zappi, M. E. (2020). Adsorption kinetic modeling using pseudo-first order and pseudo-second order rate laws: A review. *Cleaner Engineering and Technology*, *1*(December), 100032. https://doi.org/10.1016/j.clet.2020.100032

Roa, K., Oyarce, E., Boulett, A., ALSamman, M., Oyarzún, D., Pizarro, G. D. C., & Sánchez, J. (2021). Lignocellulose-based materials and their application in the removal of dyes from water: A review. *Sustainable Materials and Technologies*, *29*(June), e00320. https://doi.org/10.1016/j.susmat.2021.e00320

Saadi, R., Saadi, Z., Fazaeli, R., & Fard, N. E. (2015). *Monolayer and multilayer* *adsorption isotherm models for sorption from aqueous media*. *32*(5), 787–799. https://doi.org/10.1007/s11814-015-0053-7

Saha, B., Chowdhury, S., Sanyal, D., Chattopadhyay, K., & Suresh Kumar, G. (2018). Comparative Study of Toluidine Blue O and Methylene Blue Binding to Lysozyme and Their Inhibitory Effects on Protein Aggregation. *ACS Omega*, *3*(3), 2588–2601. https://doi.org/10.1021/acsomega.7b01991

Salimi, A., & Roosta, A. (2019). Experimental solubility and thermodynamic aspects of methylene blue in different solvents. *Thermochimica Acta*, *675*(March), 134–139. https://doi.org/10.1016/j.tca.2019.03.024

Sardar, M., Manna, M., Maharana, M., & Sen, S. (2021). *Remediation of Dyes from Industrial Wastewater Using Low-Cost Adsorbents* (pp. 377–403). https://doi.org/10.1007/978-3-030-47400-3_15

Sarkar, N., Ghosh, S. K., Bannerjee, S., & Aikat, K. (2012). Bioethanol production from agricultural wastes : An overview. *Renewable Energy*, *37*(1), 19–27. https://doi.org/10.1016/j.renene.2011.06.045

Sartape, A. S., Mandhare, A. M., Jadhav, V. V., Raut, P. D., Anuse, M. A., & Kolekar, S. S. (2017). Removal of malachite green dye from aqueous solution with adsorption technique using Limonia acidissima (wood apple) shell as low cost adsorbent. *Arabian Journal of Chemistry*, *10*, S3229–S3238. https://doi.org/10.1016/j.arabjc.2013.12.019

Schirmer, R. H., Coulibaly, B., Stich, A., Scheiwein, M., Merkle, H., Eubel, J., Becker, K., Becher, H., Müller, O., Zich, T., Schiek, W., & Kouyaté, B. (2003). Methylene blue as an antimalarial agent. *Redox Report*, *8*(5), 272–275. https://doi.org/10.1179/135100003225002899

Senthil Kumar, P., Fernando, P. S. A., Ahmed, R. T., Srinath, R., Priyadharshini, M., Vignesh, A. M., & Thanjiappan, A. (2014). EFFECT OF TEMPERATURE ON THE ADSORPTION OF METHYLENE BLUE DYE ONTO SULFURIC ACID–TREATED ORANGE PEEL. *Chemical Engineering Communications*, *201*(11), 1526–1547. https://doi.org/10.1080/00986445.2013.819352

Shi, G., Shen, Q., Zhang, C., Ma, J., Mohammed, A., & Zhao, H. (2018). Efficacy and

Safety of Gabapentin in the Treatment of Chronic Cough: A Systematic Review. *Tuberculosis and Respiratory Diseases*, *81*(3), 167. https://doi.org/10.4046/trd.2017.0089

Singh, K., & Arora, S. (2011). Removal of Synthetic Textile Dyes From Wastewaters: A Critical Review on Present Treatment Technologies. *Critical Reviews in Environmental Science and Technology*, *41*(9), 807–878. https://doi.org/10.1080/10643380903218376

Sriplai, N., & Pinitsoontorn, S. (2021). Bacterial cellulose-based magnetic nanocomposites: A review. *Carbohydrate Polymers*, *254*, 117228. https://doi.org/10.1016/j.carbpol.2020.117228

Sun, S., Sun, S., Cao, X., & Sun, R. (2016). The role of pretreatment in improving the enzymatic hydrolysis of lignocellulosic materials. *Bioresource Technology*, *199*(September), 49–58. https://doi.org/10.1016/j.biortech.2015.08.061

Sun, X., Lv, X., Han, C., Bai, L., Wang, T., & Sun, Y. (2022). Fabrication of Polyethyleneimine-Modified Nanocellulose/Magnetic Bentonite Composite as a Functional Biosorbent for Efficient Removal of Cu(II). *Water*, *14*(17), 2656. https://doi.org/10.3390/w14172656

Tan, I. A. W., Ahmad, A. L., & Hameed, B. H. (2008). Adsorption of basic dye using activated carbon prepared from oil palm shell: batch and fixed bed studies. *Desalination*, *225*(1–3), 13–28. https://doi.org/10.1016/j.desal.2007.07.005

Thakur, V., Guleria, A., Kumar, S., Sharma, S., & Singh, K. (2021). Recent advances in nanocellulose processing, functionalization and applications: a review. *Materials Advances*, *2*(6), 1872–1895. https://doi.org/10.1039/D1MA00049G

Thomas, B., Raj, M. C., Athira, B., Rubiyah, H., Joy, J., Drisko, G. L., & Sanchez, C. (2019). *Nanocellulose , a Versatile Green Platform : From Biosources to Materials and Their Applications Nanocellulose a Versatile Green Platform : From Biosources to Materials and their Applications*.

Tixier, C., Singer, H. P., Oellers, S., & Müller, S. R. (2003). Occurrence and Fate of Carbamazepine, Clofibric Acid, Diclofenac, Ibuprofen, Ketoprofen, and Naproxen in Surface Waters. *Environmental Science & Technology*, *37*(6), 1061–1068.

https://doi.org/10.1021/es025834r

Tripathi, N. (2019). *comprehensive review by : Cationic and anionic dye adsorption by agricultural solid wastes : A comprehensive review by : January 2013*. https://doi.org/10.9790/5736-5391108

Tsade, H., Anshebo, S. T., & Sabir, F. K. (2021). *Preparation and Characterization of Functionalized Cellulose Nanomaterials (CNMs) for Pb (II) Ions Removal from Wastewater*. *2021*(Ii).

Uddin, M. K., & Nasar, A. (2020). Decolorization of Basic Dyes Solution by Utilizing Fruit Seed Powder. *KSCE Journal of Civil Engineering*, *24*(2), 345–355. https://doi.org/10.1007/s12205-020-0523-2

Uddin, M. T., Rahman, M. A., Rukanuzzaman, M., & Islam, M. A. (2017). A potential low cost adsorbent for the removal of cationic dyes from aqueous solutions. *Applied Water Science*, *7*(6), 2831–2842. https://doi.org/10.1007/s13201-017-0542-4

Voisin, H., Bergström, L., Liu, P., & Mathew, A. (2017). Nanocellulose-Based Materials for Water Purification. *Nanomaterials*, *7*(3), 57. https://doi.org/10.3390/nano7030057

VTD Alencar, L., Passos, L. M., Soares, C. M., Lima, A. S., & Souza, R. L. (2020). Curr Trends Fashion Technol Textile Eng Efficiency Method for Methylene Blue Recovery Using Aqueous Two-Phase Systems based on Cholinium-Ionic Liquids. *Curr Trends Fashion Technol Textile Eng*, *6*(1), 20–22. https://doi.org/10.19080/CTFTTE.2020.06.555678

Wakkel, M., Khiari, B., & Zagrouba, F. (2019). Textile wastewater treatment by agro-industrial waste: Equilibrium modelling, thermodynamics and mass transfer mechanisms of cationic dyes adsorption onto low-cost lignocellulosic adsorbent. *Journal of the Taiwan Institute of Chemical Engineers*, *96*(xxxx), 439–452. https://doi.org/10.1016/j.jtice.2018.12.014

Wallyn, Anton, & Vandamme. (2019). Synthesis, Principles, and Properties of Magnetite Nanoparticles for In Vivo Imaging Applications—A Review. *Pharmaceutics*, *11*(11), 601. https://doi.org/10.3390/pharmaceutics11110601

Wang, B., & Sain, M. (2007). Dispersion of soybean stock-based nanofiber in a plastic matrix. *Polymer International*, *56*(4), 538–546. https://doi.org/10.1002/pi.2167

Wang, H., Gao, H., Chen, M., Xu, X., Wang, X., Pan, C., & Gao, J. (2016). Microwave-assisted synthesis of reduced graphene oxide/titania nanocomposites as an adsorbent for methylene blue adsorption. *Applied Surface Science*, *360*, 840–848. https://doi.org/10.1016/j.apsusc.2015.11.075

Wang, H., Wang, J., Fang, Z., Wang, X., & Bu, H. (2010). Enhanced bio-hydrogen production by anaerobic fermentation of apple pomace with enzyme hydrolysis. *International Journal of Hydrogen Energy*, *35*(15), 8303–8309. https://doi.org/10.1016/j.ijhydene.2009.12.012

Wang, T., & Zhao, Y. (2021). Optimization of bleaching process for cellulose extraction from apple and kale pomace and evaluation of their potentials as film forming materials. *Carbohydrate Polymers*, *253*(October 2020), 117225. https://doi.org/10.1016/j.carbpol.2020.117225

Wang, Y., Wei, X., Li, J., Wang, F., Wang, Q., Zhang, Y., & Kong, L. (2017). Homogeneous isolation of nanocellulose from eucalyptus pulp by high pressure homogenization. *Industrial Crops and Products*, *104*, 237–241. https://doi.org/10.1016/j.indcrop.2017.04.032

Weiss, N., Börjesson, J., Pedersen, L. S., & Meyer, A. S. (2013). Enzymatic lignocellulose hydrolysis: Improved cellulase productivity by insoluble solids recycling. *Biotechnology for Biofuels*, *6*(1), 5. https://doi.org/10.1186/1754-6834-6-5

Wulandari, W. T., Rochliadi, A., & Arcana, I. M. (2016). Nanocellulose prepared by acid hydrolysis of isolated cellulose from sugarcane bagasse. *IOP Conference Series: Materials Science and Engineering*, *107*(1), 012045. https://doi.org/10.1088/1757-899X/107/1/012045

Wuletaw, M. (2018). Public discourse on Khat (Catha edulis) production in Ethiopia: Review. *Journal of Agricultural Extension and Rural Development*, *10*(10), 192–201. https://doi.org/10.5897/JAERD2018.0984

Xu, S., & Lee, T. R. (2021). Fe 3 O 4 Nanoparticles : Structures , Synthesis , Magnetic Properties , Surface Functionalization , and. *Appl. Sci.*, *11*, 11301.

Yagub, M. T., Sen, T. K., Afroze, S., & Ang, H. M. (2014). Dye and its removal from aqueous solution by adsorption: A review. *Advances in Colloid and Interface Science*, *209*, 172–184. https://doi.org/10.1016/j.cis.2014.04.002

Yan, H., Tao, X., Yang, Z., Li, K., Yang, H., Li, A., & Cheng, R. (2014). Effects of the oxidation degree of graphene oxide on the adsorption of methylene blue. *Journal of Hazardous Materials*, *268*, 191–198. https://doi.org/10.1016/j.jhazmat.2014.01.015

Ye, Z., Liu, Y., Jin, X., Wu, Y., Zhao, H., Gao, T., Deng, Q., Cheng, J., Lin, J., & Tong, Z. (2024). International Journal of Biological Macromolecules A β -binding with alcohol dehydrogenase drives Alzheimer ' s disease pathogenesis : A review. *International Journal of Biological Macromolecules*, *264*(P2), 130580. https://doi.org/10.1016/j.ijbiomac.2024.130580

Yıldız, E., Saçmacı, Ş., Kartal, Ş., & Saçmacı, M. (2016). A new chelating reagent and application for coprecipitation of some metals in food samples by FAAS. *Food Chemistry*, *194*(July), 143–148. https://doi.org/10.1016/j.foodchem.2015.07.084

Yohannes, H., & Elias, E. (2017). Contamination of Rivers and Water Reservoirs in and Around Addis Ababa City and Actions to Combat It. *Environment Pollution and Climate Change*, *01*(02). https://doi.org/10.4172/2753-458X.1000116

Yuan, N., Cai, H., Liu, T., Huang, Q., & Zhang, X. (2019). Adsorptive removal of methylene blue from aqueous solution using coal fly ash-derived mesoporous silica material. *Adsorption Science & Technology*, *37*(3–4), 333–348. https://doi.org/10.1177/0263617419827438

Zamboni Schiavon, J., & de Oliveira Andrade, J. J. (2023). Comparison between alternative chemical treatments on coir fibers for application in cementitious materials. *Journal of Materials Research and Technology*, *25*, 4634–4649. https://doi.org/10.1016/j.jmrt.2023.06.210

Zhang, Y., Li, J., Ma, N., Meng, Z., & Sui, G. (2019). Processing cellulose@Fe3O4 into mechanical, magnetic and biodegradable synapse-like material. *Composites Part B: Engineering*, *177*(June), 107432. https://doi.org/10.1016/j.compositesb.2019.107432

Zhang, Y. P., Ding, S., Mielenz, J. R., Cui, J., Elander, R. T., Laser, M., Himmel, M. E., Mcmillan, J. R., Lynd, L. R., Systems, B., & Tech, V. (2007). *Fractionating*

Recalcitrant Lignocellulose at Modest Reaction Conditions. *97*(2), 214–223. https://doi.org/10.1002/bit

Zhao, Y., Lei, H., Liu, Y., Ruan, R., Qian, M., Huo, E., Zhang, Q., Huang, Z., Lin, X., Wang, C., Mateo, W., & Villota, E. M. (2020). Microwave-assisted synthesis of bifunctional magnetic solid acid for hydrolyzing cellulose to prepare nanocellulose. *Science of The Total Environment*, *731*, 138751. https://doi.org/10.1016/j.scitotenv.2020.138751

Zhou, Y., Lu, J., Zhou, Y., & Liu, Y. (2019). Recent advances for dyes removal using novel adsorbents: A review. *Environmental Pollution (Barking, Essex : 1987)*, *252*(Pt A), 352–365. https://doi.org/10.1016/j.envpol.2019.05.072